Reviews in Mineralogy & Geochemistry
Vol. 56, pp. 347-398, 2004

Epidote Minerals in High P/T Metamorphic Terranes: Subduction Zone and High- to Ultrahigh-Pressure Metamorphism

M. Enami

Department of Earth and Planetary Sciences
Nagoya University
Nagoya 464-8602, Japan

J. G. Liou and C. G. Mattinson

Department of Geological and Environmental Sciences
Stanford University
Stanford, California 94305, U.S.A.

INTRODUCTION

Epidote minerals—the monoclinic epidote group minerals together with the orthorhombic polymorph zoisite—are important Ca-Al-silicates in many metabasites, metapelites and metacherts that are characterized by high P/T ratios. Such high P/T ratios are typical for subduction zones and the high-pressure (HP) and ultrahigh-pressure (UHP) metamorphism during continent-continent collisions (e.g., Liou 1973, 1993). All of these P-T conditions can be described by geothermal gradients between 5 and 20°C/km, that therefore provide a rough framework for the P-T conditions covered by this review (Fig. 1). Depending on the actual thermal structure of a subduction zone, the subducting plate will encounter subgreenschist, greenschist, blueschist, epidote-amphibolite, amphibolite, HP granulite, and/or eclogite facies conditions during its travel down into the mantle (Fig. 1). The P-T regime of the eclogite facies can further be subdivided into amphibole eclogite, epidote eclogite, lawsonite eclogite, and dry eclogite facies (Fig. 1). HP metamorphism refers to metamorphic pressure in excess of ~1.0 GPa and includes parts of the blueschist, epidote-amphibolite, and HP granulite facies as well as the eclogite facies (Fig. 1). UHP refers to the metamorphism of crustal rocks (both continental and oceanic) at P high enough to crystallize the index minerals coesite and/or diamond. HP and UHP metamorphism are separated conveniently by the quartz-coesite equilibrium which implies a minimum $P > 2.7$ GPa at $T > 600$°C for UHP metamorphism (Fig. 1). The equilibrium boundary for the graphite-diamond transition can be used to further subdivide the UHP region into diamond-grade and coesite-grade. The stability of coesite and other UHP minerals in a metamorphic regime requires abnormally low temperatures at depths greater than 100 km. Such environments can be attained only by the subduction of cold oceanic crust-capped lithosphere ± pelagic sediments or of continental crust.

Epidote minerals occur as characteristic phases in the greenschist, blueschist and epidote-amphibolite facies and in the lawsonite and epidote eclogite facies. They have also been reported from coesite-bearing eclogites (e.g., Liou 1993). Occurrence of polycrystalline clinozoisite aggregates, interpreted as pseudomorphs after former lawsonite porphyroblasts, are identified in HP rocks from several localities (e.g., Krogh 1982; Droop 1985; Gomez-Pugnaire

1529-6466/04/0056-0008$10.00

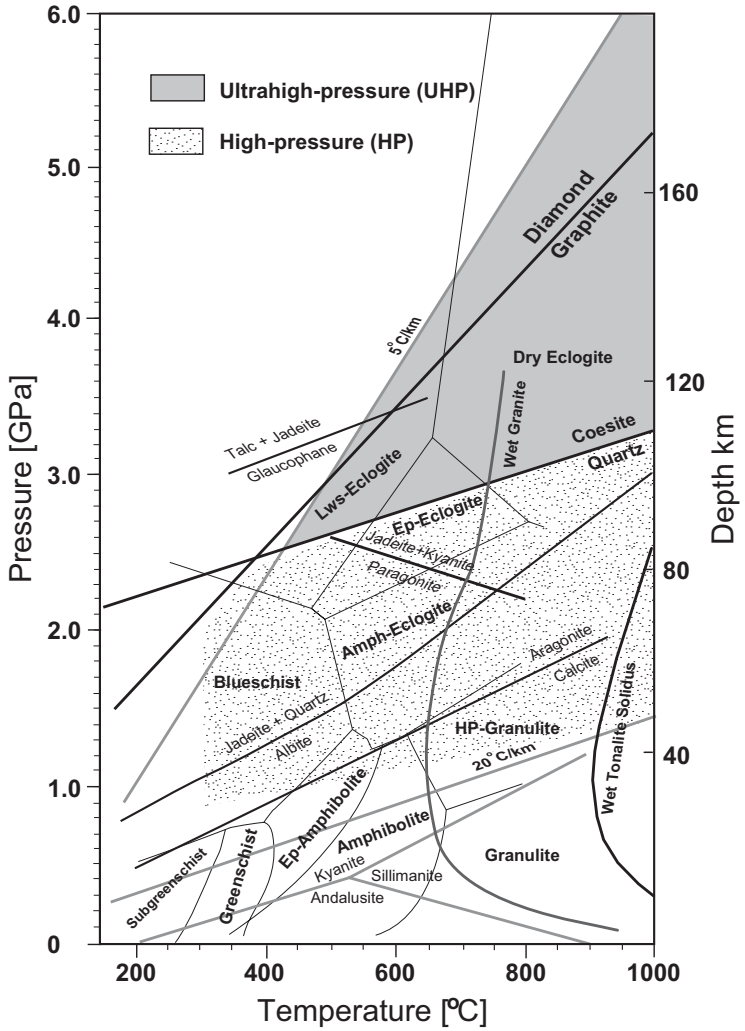

Figure 1. *P-T* regimes of UHP and HP metamorphism. The blank area below ≈ 1 GPa is the field of medium to low *P* metamorphism. Geotherms of 5°C/km and 20°C/km are indicated (modified from Fig. 1 of Liou and Zhang 2002).

et al. 1985) and were recently described in Dabie quartz eclogites with peak *P-T* estimated at 2.4 GPa and 700°C (e.g., Castelli et al. 1998). At appropriate bulk rock composition and f_{O_2} and X_{CO_2} conditions, epidote minerals might even coexist with microdiamond (+ coesite) as in the diamond-grade UHP rocks of the Kokchetav Massif where metamorphic microdiamond was first documented (Sobolev and Shatsky 1990).

The composition of epidote minerals is highly variable and mainly controlled by temperature, pressure, oxygen fugacity (f_{O_2}), and bulk rock composition. In metabasites they tend to be more Fe-rich than in metapelites, which commonly contain graphite. Metacherts, which generally recrystallize under much higher f_{O_2} than other rock-types, typically contain

epidote or piemontite. The compositional range of epidote minerals in terms of their X_{Fe} [Fe^{3+}/($Al + Cr + Fe^{3+} + Mn^{3+}$)] value enlarges towards the low X_{Fe}-side with increasing metamorphic grade. Enlargement of the compositional field combined with the two-phase loop between zoisite and clinozoisite leads to the common occurrence of zoisite in HP metamorphic rocks, especially in eclogites.

Another compositional variation of epidote minerals important for the rocks reviewed in this chapter is the element proportions in their largest A(2)-site. High concentrations of Sr and REE in epidote minerals reported from HP and UHP terranes strongly suggest that (1) zoisite and epidote are the most important Sr and REE reservoirs at HP and UHP conditions where they are a major Ca-Al-silicate, and (2) their stability strongly controls the recycling of Sr and REE in HP-UHP environments (e.g., Sorensen and Grossman 1989; Nagasaki and Enami 1998).

Major themes to be addressed

This chapter focuses mainly on modes of occurrences of zoisite, clinozoisite-epidote and piemontite in various rock types from selected subduction zones and HP to UHP metamorphic terranes. The amount of information on these rocks has increased dramatically during the last 20 years and it is virtually impossible to completely review all. We therefore restrict this review mainly to those localities where we have our own experience, and add some information from other localities. Epidote minerals in metamorphic rocks that followed classical barrowian- or Buchan-type metamorphism are reviewed by Grapes and Hoskin (2004). Nevertheless, as the *P-T* conditions encountered during subduction zone and Barrovian-type metamorphism are not thus distinct in the *P-T* range of the greenschist, blueschist, to epidote-amphibolite facies transition, some overlaps between Grapes and Hoskin (2004) and this chapter were found to be unavoidable. As subduction zone metamorphism represents also a potential prograde path of many HP and UHP rocks we will first review some selected and well studied examples of subduction zone metamorphism and then prograde into the field of the peculiar HP and UHP metamorphic rocks.

Specifically, this chapter deals with the following major subjects: (1) Prograde sequences from lawsonite to epidote zone blueschists and the corresponding epidote-forming reactions are described from the Franciscan, New Caledonian and Sanbagawa metamorphic rocks; these examples are used to illustrate the role of epidote minerals in typical subduction zone metamorphic successions. (2) Phase relations of zoisite-bearing assemblages in calcareous metasediments are briefly reviewed for eclogite facies rocks in the European Alps. (3) The control of bulk rock composition on paragenesis and compositions of UHP phases is exemplified by various zoisite-bearing UHP eclogites from Dabie (central China) with an AFM diagram. (4) The common break down of plagioclase in HP and UHP rocks in the presence of H_2O to form the assemblage zoisite + kyanite + sodic clinopyroxene + quartz is illustrated in some HP to UHP coronitic metagranites and metagabbros. (5) The common but selective occurrence of epidote minerals in Sulu-Dabie eclogite, quartzite and gneiss may be related to the oxidation of supracrustal rocks by a fossil hydrothermal system. (6) The pseudomorphic replacements of epidote/zoisite + amphibole + biotite + sodic plagioclase after garnet and of zoisite + albite after kyanite as indicators for a metasomatic and retrograde overprint during exhumation are described using kyanite-phengite-coesite eclogites from Dabie. (7) The coexistence of lawsonite and epidote in some HP metabasites is related to bulk composition, f_{O_2} and metastable persistence. (8) Composition of epidote minerals from buffered assemblages is sensitive to *P*, *T* and f_{O_2}, and its use as a geobarometer or geothermometer is discussed. (9) Epidote minerals are a key to discuss fluid-rock interaction and partial melting of metamorphic rocks at high-*P* conditions. (10) Unusually high Sr and REE contents in epidote minerals including allanite suggest that they are the main reservoirs of these elements in subduction zones and HP to UHP environments. (11) Sector-zoning of zoisite and epidote and their petrological and mineralogical significance is also briefly discussed.

Mineral abbreviations employed in this chapter are after Kretz (1983) and Miyashiro (1994) other than Amph (amphibole), Bar (barroisite), Cro (crossite), Coe (coesite), Coe-ps (quartz pseudomorph after coesite), Dia (diamond), Fgln (ferroglaucophane), Mrb (magnesioriebeckite), Sr-Pie (strontiopiemontite) and Wnc (winchite).

EPIDOTE MINERALS IN A TYPICAL BLUESCHIST FACIES METAMORPHISM: THE FRANCISCAN COMPLEX/CALIFORNIA

Major lithologies of the Franciscan Complex of the California Coast Range, the classic example of a subduction complex, are metaclastic rocks plus minor metacherts and metabasites. These rocks were subjected to Cretaceous blueschist-facies metamorphism and contain combinations of pumpellyite, lawsonite, epidote, phengite, albite, chlorite, sodic amphibole, quartz and titanite. Lawsonite and minor epidote and pumpellyite are the dominant Ca-Al-silicates. Epidote is restricted to the metabasites and has not been recognized as a neoblastic phase in metagraywackes (e.g., Ernst 1965; Ernst et al. 1970; Jayko et al. 1986). Within the *P-T* conditions of the blueschist facies, characteristic metabasite assemblages contain lawsonite at lower temperature and epidote at higher temperature together with aragonite and jadeitic clinopyroxene + quartz in addition to sodic amphibole. Franciscan epidote-bearing rocks include greenstone, greenschist, blueschist, high-grade blueschist "knockers" and eclogites. Many eclogite blocks have experienced a counter-clockwise *P-T* path starting from epidote-amphibolite through eclogite- to blueschist-facies re-equilibration (Moore 1984; Krogh et al. 1994). Epidote also occurs in both pre- and post-eclogite facies stages.

The following discussion focuses on paragenesis and compositions of epidote in blueschists and eclogites from Ward Creek of the Central belt as the most representative Franciscan epidote-bearing metabasites occur in this area. This area has been intensively studied since aragonite was first identified here (Coleman and Lee 1963; Liou and Maruyama 1987; Maruyama and Liou 1987, 1988; Oh and Liou 1990; Oh et al. 1991; Shibakusa and Maekawa 1997; Banno et al. 2000).

Prograde zoning of Franciscan metabasite in Ward Creek of the Cazadero region

The Jurassic-Cretaceous blueschist sequence of Cazadero lies within the Central Franciscan belt of the northern California Coast Range. Coleman and Lee (1963) classified the metabasites into 4 types: (I) unmetamorphosed, (II) metamorphosed and non-foliated, (III) metamorphosed and foliated, and (IV) coarsely crystalline tectonic blocks. Type II and III metabasites are the most abundant and are continuously exposed for more than 2 km in Ward Creek. Within the metabasites three prograde metamorphic zones (lawsonite, pumpellyite, and epidote zone) and their mineral paragenesis were mapped (Fig. 2; Maruyama and Liou 1988; Oh et al. 1991). All metabasites contain minor quartz, white mica, albite, chlorite, titanite, and aragonite. Both the lawsonite and pumpellyite zones are equivalent to the Type II non-foliated metabasite of Coleman and Lee (1963). The epidote zone includes Type III blueschists, *in situ* eclogite and Type IV tectonic blocks. In some Type III epidote-zone blueschists garnet occurs together with omphacite, epidote, glaucophane and other epidote-zone minerals, indicating the onset of transition to the eclogite facies (Oh and Liou 1990).

Epidote zone metabasites are characterized by the assemblages epidote + clinopyroxene + two amphiboles + chlorite, lawsonite + pumpellyite + actinolite + chlorite and epidote + pumpellyite + two amphiboles + chlorite depending on bulk rock Fe_2O_3 content. With increasing grade, winchite appears, Fe-free lawsonite is stable with epidote, pumpellyite disappears, and omphacite contains a very low acmite component. The common assemblages are epidote + winchite + lawsonite and lawsonite + omphacite + winchite. Epidote becomes Al-rich where lawsonite is no longer stable. Hence epidote + glaucophane + omphacite + garnet is characteristic and was named high-epidote zone eclogite (Oh et al. 1991).

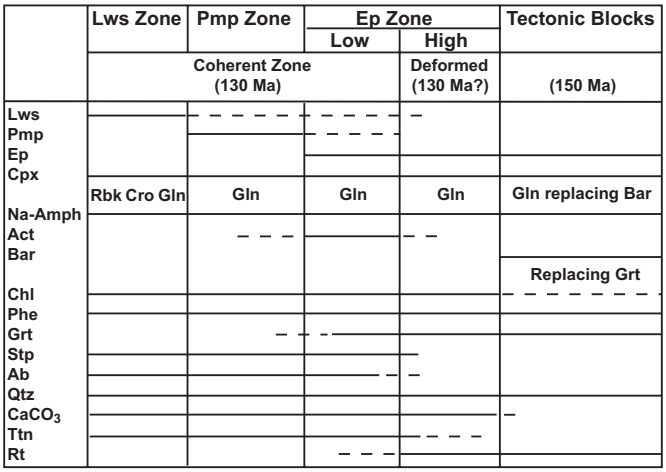

Figure 2. Mineral paragenesis in Ward Creek metabasites/Franciscan, California (modified from Table 2 of Oh et al. 1991). Three metamorphic zones increasing from left to right occur in a continuous exposure in Ward Creek (Maruyama and Liou 1988) and tectonic blocks are enclosed within serpentinite or in epidote-zone metabasites.

Serpentinite mélange of the Franciscan Complex contains Type IV tectonic blocks including eclogite, high-grade blueschist, and garnet amphibolite; these rocks are different from the epidote-zone metabasites mentioned above. Epidote is abundant in these rocks ranging from 15 to 29 vol% (mineral paragenesis in Fig. 2, compiled from Tables 3 and 4 of Oh et al. 1991). These rocks are older (150 Ma) than type III metabasites (130 Ma) (Lee et al. 1964; Coleman and Lanphere 1971).

Paragenesis and composition of major phases in Ward Creek blueschist and eclogitic rocks and *P-T* estimates are discussed in detail using a modified epidote-projection ACF diagram (Liou and Maruyama 1987; Maruyama and Liou 1987, 1988; Oh et al. 1991). The lawsonite zone appears to be stable at $T < 200$°C in a pressure range of 0.4–0.65 GPa; the pumpellyite zone between 200-290°C and the epidote zone above 290°C at 0.65 to 0.9 GPa (Maruyama and Liou 1987). The *P-T* estimate for *in situ* eclogitic schist is 290°C $< T <$ 350°C, $0.8 < P <$ 0.9 GPa, whereas that of type IV eclogite is 500°C $< T <$ 540°C, $P >$1.0–1.15 GPa.

Epidote texture and composition

Maruyama and Liou (1987) describe two distinct modes of epidote occurrence in Type III epidote-zone metabasite. The first type is fine-grained epidote aggregates that replace primary augite phenocrysts. Individual epidote grains have an irregular habit and a dusty appearance. Some grains contain abundant inclusions of titanite, clinopyroxene and minor pumpellyite. The textural relations, the inverse modal proportion of epidote and clinopyroxene, and the sudden decrease in the modal abundance of both clinopyroxene + pumpellyite at the onset of the epidote zone suggest that the granular epidote have formed by a reaction such as clinopyroxene + pumpellyite = epidote + amphibole. This epidote type lacks the pleochroic colors for common epidote due to small grain size and constitutes less than 5 vol%; it is not surprising that Coleman and Lee (1962) did not identify epidote in Type III metabasite. The second type of epidote occurs as rims around xenoblastic, coarse-grained pumpellyite and lawsonite. This subidioblastic epidote is free from inclusions. Although lawsonite is abundant and coarse-grained in some epidote-zone metabasites, textural relations suggest that lawsonite is not in equilibrium with epidote. A third type of epidote can be described for the

Type III epidote-zone *in situ* eclogites. This is coarse-grained, idioblastic, and exhibits the characteristic interference colors.

Representative analyses of epidote from blueschists and eclogites from this area are listed in Table 1; their X_{Fe} content is plotted against the metamorphic grade in Figure 3. Epidote contains low total Mn (0.05–0.6 wt% MnO) and TiO_2 and negligible amounts of Na_2O, MgO and Cr_2O_3. Epidote in blueschists varies substantially in composition, but has consistently higher X_{Fe} in the core than in the rim suggesting progressive growth with increasing temperature. However, the overall trend with increasing grade does not show such a relationship (Fig. 3). The epidote core has X_{Fe} = 0.18 to 0.22 whereas the epidote rim has X_{Fe} = 0.13 to 0.17. Epidote of *in situ* eclogites has the same core to rim relation as that in the associated blueschists. However, it has generally higher X_{Fe} (0.24 to 0.29) and MnO contents (0.37 to 0.67 wt%; Fig. 3) suggesting higher Fe^{3+} and Mn in the whole rock, which is consistent with the occurrence of crossite and Mn-rich garnet (Oh et al. 1991). Contrary to epidote from the Type III epidote-zone rocks, epidote from Type IV tectonic blocks has the inverse core to rim relation with higher Fe^{3+} content in the rim than in the core. This can be interpreted as retrograde re-equilibration at lower *T* during later blueschist facies overprint.

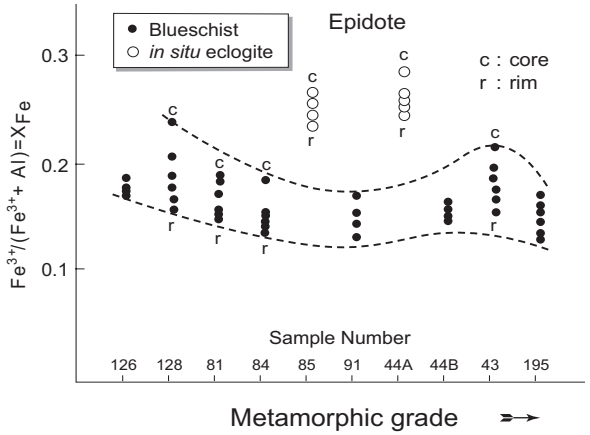

Figure 3. Compositional ranges of epidote from blueschist, and *in-situ* eclogite from Ward Creek. Both core and rim compositions are shown and they are arranged according to the inferred metamorphic grade for the blueschist (modified from Fig. 10 of Maruyama and Liou 1988).

EPIDOTE MINERALS IN LAWSONITE BLUESCHIST-ECLOGITE FACIES METAMORPHISM: PAM-OUÉGOA-POUÉBO REGION/NEW CALEDONIA

Palaeogene high *P*/*T* metamorphic rocks are exposed in an elongate anticlinal range of northwestern New Caledonia (e.g., Brothers 1974; Black 1977). Based on the mineral paragenesis of metapelites, Yokoyama et al. (1986) grouped them into five zones of increasing metamorphic grade: low-grade lawsonite, Mn-garnet, lawsonite-epidote transition, epidote, and omphacite zones. Clarke et al. (1997) divided the metamorphic rocks into two terranes: (1) the structurally higher Diahot terrane of blueschist facies metasediments and metavolcanics; and (2) the structurally lower Pouébo terrane of eclogites and their hydration product glaucophanite and rare quartzite. The Diahot terrane is subdivided into a lower-grade ferroglaucophane-lawsonite zone and higher-grade albite-epidote-omphacite zone. Schists of the ferroglaucophane-lawsonite zone have mineral assemblages similar to the

Table 1. Representative analyses of epidote minerals from the Franciscan complex.

Locality	Ward Creek							Diablo Range		Oregon	
Rock Type	IEc	EBl	EBl	EBl	HEEc	GAm	VIEc	EBl	EBl	HBl	Hs
Sample	W-85	W-91	W-91	W-43	W-06	W-32	WT-73	GL1	GL1	Ore11	Ore8
Mineral	Ep	Ep (c)	Ep (r)	Ep	Ep	Ep	Ep	Ep (c)	Ep (r)	Ep (r)	Ep (r)
SiO_2	37.55	38.70	38.99	38.06	36.63	38.53	38.09	37.2	38.2	38.11	37.77
TiO_2	0.11	0.11	0.12	0.02	0.00	0.15	0.19	0.1	0.1	0.08	0.07
Al_2O_3	24.40	26.69	28.13	27.23	24.86	26.17	26.28	22.5	25.8	27.77	25.93
Cr_2O_3	0.07	0.07	0.00	0.12	0.00	0.00	0.00	n.d.	n.d.	n.d.	n.d.
Fe_2O_3*	11.26	8.39	6.71	8.07	12.71	8.82	7.41	15.5	11.4	8.80	11.20
MnO	0.51	0.30	0.08	0.10	0.44	0.04	0.10	0.3	0.3	0.12	0.18
MgO	0.04	0.17	0.00	0.13	0.00	0.07	0.08	n.d.	0.1	0.01	0.04
CaO	22.16	22.89	23.21	22.04	22.86	23.22	23.24	22.8	22.9	23.76	23.59
Na_2O	n.d.	0.14	n.d.	0.00	n.d.	n.d.	n.d.	n.d.	0.2	n.d.	n.d.
K_2O	n.d.	0.00	n.d.	0.00	n.d.	n.d.	n.d.	n.d.	n.d.	n.d.	n.d.
Total	96.10	97.46	97.24	95.77	97.50	97.00	95.39	98.40	99.00	98.65	98.78
X_{Fe}**	0.23	0.17	0.13	0.16	0.25	0.18	0.15	0.31	0.22	0.17	0.22
Ref.	O91	M88	M88	M88	O91	O91	O91	M84	M84	M89	M89

* Total Fe as Fe_2O_3, $X_{Fe} = Fe^{3+}/(Al + Cr + Fe^{3+} + Mn^{3+})$.

Abbreviations of rock-types: IEc, *in-situ* eclogite; EBl, epidote-blueschist; HEEc, HE-eclogite; GAm, garnet-amphibolite; VIEc, type VI-eclogite; Hs, hornblende schist.

Other abbreviations: c, crystal core; r, crystal rim; n.d., not determined.

References: O91, Oh et al. (1991); M88, Maruyama and Liou (1988); M84, Moore (1984); M89, Moore and Blake (1989).

Mn-garnet zone of Yokoyama et al. (1986) and their peak *P*/*T* conditions are estimated at 0.7–0.9 GPa/340–460°C (Clarke et al. 1997). Schists of the albite-epidote-omphacite zone are significantly coarser grained than those in the ferroglaucophane-lawsonite zone and are equivalent in mineral paragenesis to schists of the lawsonite-epidote transition, epidote, and the lower-grade part of the omphacite zone of Yokoyama et al. (1986). Their estimated peak *P*/*T* conditions are 1.1–1.4 GPa/530-610°C. The eclogite paragenesis of the Pouébo terrane roughly correspond to those of the omphacite zone of Yokoyama et al. (1986) with estimated peak *P*/*T* conditions of 2.1–2.7 GPa/~600°C (Clarke et al. 1997). Clarke et al. (1997) recognized three rock-types of eclogite facies having bulk rock compositions consistent with protoliths of basalt (Type I), gabbro cumulate (Type II), and chert (Type III), respectively. The following review is mainly based upon data of Yokoyama et al. (1986) and Clarke et al. (1997) unless otherwise noted.

Epidote-bearing mineral assemblages

Epidote minerals are common in metabasites and metapelites from the albite-epidote-omphacite zone of the Diahot terrane and in eclogites of the Pouébo terrane, but are absent in meta-acidite. As epidote minerals are unstable in the lower-grade ferroglaucophane-lawsonite zone, Black (1977) proposed the following epidote-producing reactions between the ferroglaucophane-lawsonite and albite-epidote-omphacite zones:

Lws + Fe-rich Chl + Cro = Ep + Alm + Mg-rich Chl + Gln for metabasite,

Lws + Fe-rich Chl + Fgln = Ep + Alm + Mg-rich Chl + Gln and/or

Lws + Fe-rich Chl + Ab = Ep + Mg-rich Chl + Pg for metapelite.

Zoisite occurs in about 15% of the samples from the omphacite zone (Yokoyama et al. 1986) and usually coexists with Al-rich epidote. Some epidote grains are clearly retrograde products that form aggregates with chlorite and albite replacing glaucophane and paragonite. The stable epidote-bearing mineral assemblages in the different rock types as function of metamorphic grade are:

Metabasite. In the lower-grade part of the albite-epidote-omphacite zone, epidote coexists with lawsonite, omphacite, glaucophane, actinolite, chlorite, and titanite and ± phengite, albite, and/or quartz. With increasing grade lawsonite and actinolite phase out and Fe-rich garnet and rutile join the above assemblage. The eclogites of the Pouébo terrane consists of epidote with omphacite, glaucophane, barroisitic hornblende, Fe-rich garnet, paragonite, and rutile and ± titanite, phengite and/or quartz.

Metapelite. In the lower-grade part of the albite-epidote-omphacite zone, epidote coexists with lawsonite, glaucophane, Mn-rich garnet, chlorite, phengite, paragonite, titanite, rutile, quartz, graphite, and albite. With increasing grade lawsonite and Mn-rich garnet disappear and Fe-rich garnet becomes stable. In the eclogite facies metapelites of the Pouébo terrane zoisite and omphacite occur as major constituent phases, and chlorite is absent in most samples.

Meta-acidite. Epidote minerals are generally absent in meta-acidite. Black et al. (1988) discussed the relationship between bulk rock chemistry and stability of clinozoisite, omphacite, and jadeite in metamorphosed siliceous sediments at eclogite facies conditions in the ½Al-Na-Ca ternary (Fig. 4). This ternary shows that the stability of these minerals is almost exclusively a function of the $X_{Na}^{\text{whole rock}}$ [= Na/(Na + Ca)] of the host rock. Clinozoisite is restricted to $X_{Na}^{\text{whole rock}} < 0.27$, omphacite occurs in rocks with $X_{Na}^{\text{whole rock}} = 0.27\text{-}0.55$, and jadeite crystallizes in rocks with $X_{Na}^{\text{whole rock}} > 0.55$ (Fig. 4). These data indicate that epidote and zoisite become less stable with increasing $X_{Na}^{\text{whole rock}}$ of the host rock. As the meta-acidites from New Caledonia have $X_{Na}^{\text{whole rock}} > 0.55$ jadeitic pyroxene and/or its pseudomorph (albite) occur as Al-rich silicates instead of epidote and/or zoisite.

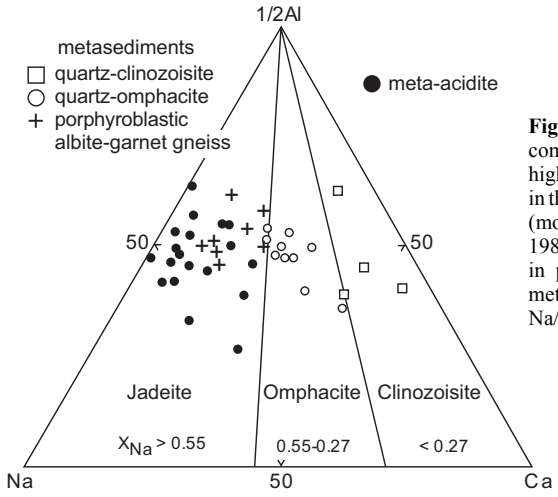

Figure 4. Relationship between bulk rock compositions and mineral assemblages in high *P*/*T* meta-acidites and metasediments in the ½Al-Na-Ca system with excess SiO_2 (modified from Fig. 4.5 of Black et al. 1988). The crystallization of clinozoisite in primary eclogite assemblages of HP metasediments is determined by the X_{Na} = Na/(Na + Ca) value of the parent rock.

Compositional range of epidote minerals

Zoisite and clinozoisite-epidote in metabasite and metapelite have been described by Yokoyama et al. (1986) and Ghent et al. (1987). The overall range in X_{Fe} of clinozoisite-epidote is 0.09 to 0.30. Zoisite displays a much smaller scatter and has generally $X_{Fe} < 0.06$. Epidote minerals in eclogitic rocks contain less Fe^{3+} than those in common metabasite; coexisting zoisite and Al-rich epidote usually occur in the Type II eclogite (gabbroic cumulate protolith) of Clarke et al. (1997). The epidote minerals in eclogite and associated metabasite contain minor amounts of TiO_2 (0.07 to 0.22 wt%), MnO (< 0.03 to 0.32 wt%) and MgO (< 0.05 to 0.13 wt%) (Ghent et al. 1987). X_{Fe} between whole rock and epidote shows a strong positive correlation (Potel et al. 2002).

Mineralogical and chemical characteristics of the New Caledonia high *P*/*T* metamorphic rocks are very similar to those reported from Sanbagawa metamorphic rocks (see below): (1) the compositional range of zoisite and clinozoisite-epidote series, (2) the common occurrence of coexisting zoisite and clinozoisite in higher-grade zone, and (3) greater abundance of zoisite in metagabbro than metabasalt.

EPIDOTE MINERALS IN GREENSCHIST/BLUESCHIST-EPIDOTE AMPHIBOLITE-ECLOGITE FACIES METAMORPHISM: THE SANBAGAWA BELT/JAPAN

The Sanbagawa high *P*/*T* metamorphic belt extends throughout the Outer Zone (the Pacific Ocean side) of Southwest Japan for a length of roughly 800 km (Miyashiro 1994). In central Shikoku the Sanbagawa belt is divided into chlorite, garnet, albite-biotite and oligoclase-biotite zones based on the matrix mineral paragenesis of pelitic schists in ascending order of metamorphic grade (Enami 1983; Higashino 1990). Peak *P*-*T* conditions of the lower-grade part of the chlorite zone correspond to that of the high-*P* pumpellyite-actinolite facies. High-grade chlorite and low-grade garnet zones approximate to the high-*P* greenschist and/or low-*P* blueschist facies, and high-grade garnet zone and albite- and oligoclase-biotite zones are equivalent to the epidote-amphibolite facies. Peak *P*/*T* conditions of the chlorite, garnet, albite-biotite and oligoclase-biotite zones are estimated at 0.5–0.7 GPa/~360°C, 0.7–1.0 GPa/

430-500°C, 0.8–1.1 GPa/470–570°C, and 0.9–1.1 GPa/580–630°C, respectively (Enami et al. 1994; Wallis et al. 2000). Within the region of epidote-amphibolite facies metamorphism of central Shikoku there are numerous ultramafic and mafic masses. The mafic rocks have protoliths of gabbro and basalt (Kunugiza et al. 1986; Takasu 1989). The mafic-ultramafic complex in the Besshi region in central Shikoku underwent extensive equilibration under epidote-amphibolite facies conditions; however, the rocks also locally preserve evidence of earlier eclogite facies metamorphism (c. 1.5–3.8 GPa/600-800°C; e.g., Takasu 1989; Wallis and Aoya 2000; Aoya 2001; Enami et al. 2004).

Composition of host rocks and epidote minerals

Epidote minerals are common and important phases throughout the different lithologies of the Sanbagawa belt. They are confirmed in almost all examined pelitic samples from the different zones although they represent only a minor phase in the individual samples (Goto et al. 2002). This extensive presence of epidote minerals is in marked contrast to the rare occurrence of epidote minerals in low to medium-grade pelitic schists of other regional metamorphic terranes (Deer et al. 1986). It probably reflects the *P-T* conditions at which epidote fulfills the role as main Ca-Al-silicate instead of calcic plagioclase. This interpretation is consistent with the occurrence of Ca-poor sodic plagioclase throughout the Sanbagawa belt.

Epidote minerals commonly show concentric zoning with decreasing or increasing X_{Fe} value from the core to margin, which are normally considered to represent prograde and retrograde growths, respectively (e.g., Otsuki and Banno 1990). Some grains, however, clearly show sector-zoning (see below). The following discussion is mainly based on data reported by Enami (1978), Otsuki (1980), Higashino et al. (1981, 1984) and Otsuki and Banno (1990).

Pelitic schists. The pelitic schists are mainly composed of quartz, sodic plagioclase, phengite, epidote, and calcite; chlorite is the main ferromagnesian mineral of the chlorite zone. In the chlorite zone, most epidote grains are too fine-grained to be positively identified using polarizing microscope (usually < 30 μm: Goto et al. 2002) and must be confirmed by SEM observation. At higher-grade, pelitic schists of the garnet zone are characterized by the coexistence of chlorite and garnet. In the albite- and oligoclase-biotite zones, these minerals are joined by biotite and hornblende/pargasite. Lawsonite appears sporadically in the lower-grade part of the chlorite zone. Zoisite coexists with Al-poor epidote in the oligoclase-biotite zone.

Zoisite has limited compositional range of X_{Fe} = 0.02–0.05 and CaO = 22.8–24.8 wt% (Fig. 5). Epidote has variable compositions ranging from epidote sensu strictu, through rare earth element (REE)-bearing epidote (Sakai et al. 1984) to allanite with CaO = 9.6–24.4 wt%. The X_{Fe} values of epidote are usually 0.10-0.20 except for epidote from chlorite zone (X_{Fe} = 0.2–0.35) and REE-bearing epidote and allanite (Fig. 5). The low X_{Fe} of epidote in garnet and higher-grade zones is probably due to low-f_{O_2} conditions inferred from the common presence of fully ordered graphite in pelitic schist (Itaya 1981, Tagiri 1985). The X_{Fe} (up to 0.40; Fig. 5), MnO (up to 1.2 wt%) and MgO (up to 0.8 wt%) of REE-epidote and allanite tend to increase with decreasing CaO. This trend suggests that some amounts of iron and manganese of REE-epidote and allanite are divalent related to the coupled substitution $REE_{+1}(Fe^{2+},Mn^{2+},Mg)_{+1}Ca_{-1}Fe^{3+}_{-1}$ (Deer et al. 1986). Most REE-epidotes occur as overgrowths on allanite, and are in turn sometimes rimmed by REE-poor epidote (Fig. 6a). REE-epidote shows grayish blue abnormal interference color and commonly forms a pleochroic halo in host biotite and chlorite, so that it is easily identified under the polarizing microscope. Average grain size of the REE-epidote systematically increases from 30 μm in the chlorite zone, through 55 μm in the garnet zone, to 65 μm in the albite-biotite zone (Sakai et al. 1984). Total REE and ThO_2 contents of most REE-epidotes are 8–15 wt% and up to 1.0 wt%, respectively. Chondrite-normalized REE-patterns for the REE-epidote are similar to those of coexisting allanite (Fig. 6b). In the Sanbagawa belt, allanite occurs

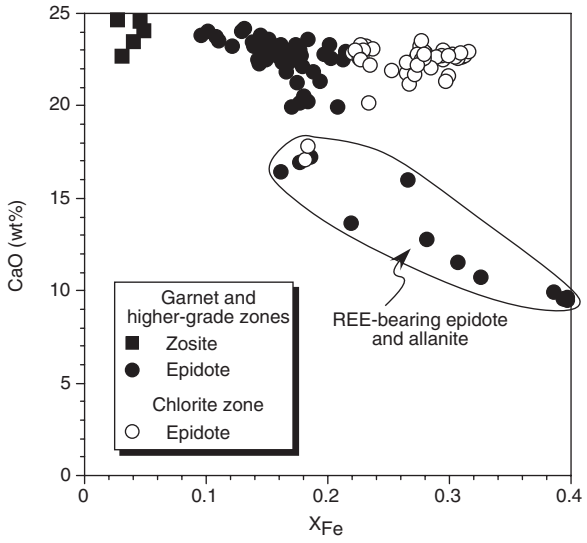

Figure 5. X_{Fe}-CaO relationship of epidote minerals in pelitic schists from the Sanbagawa belt (Higashino et al. 1981; Enami unpublished data).

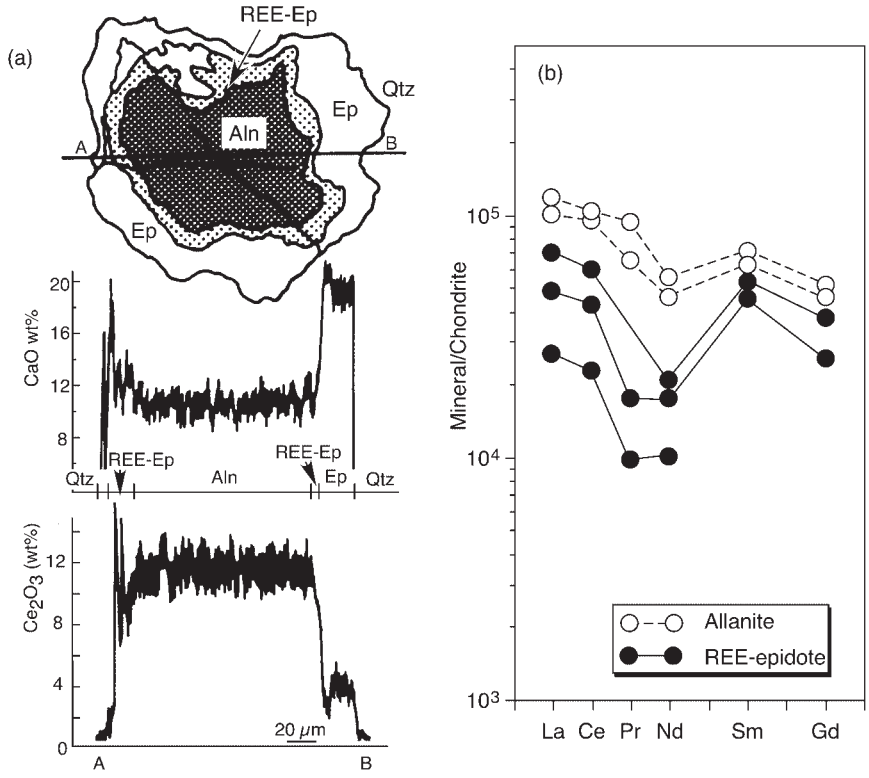

Figure 6. (a) Sketch of a epidote-allanite crystal with line scan for CaO and Ce_2O_3 and (b) Leedey chondrite (Masuda et al. 1973)-normalized REE patterns of coexisting REE-epidote and allanite in pelitic schists from the Sanbagawa belt (modified from Figs. 7 and 9 of Sakai et al. 1984).

only in metasediments and is probably detrital, and a major source of REE and Th for the crystallization of REE-epidote during prograde metamorphism.

Siliceous schist. Most siliceous schists of the Sanbagawa are metamorphosed impure cherts, and have been commonly referred to as quartz schists or quartzitic schists. Silicate minerals are similar to those of high-f_{O_2} mafic schists except for rare occurrences of sodic pyroxene (X_{Jd} = 0.02–0.35 and X_{Acm} = 0.19–0.84) and Mn-rich garnet (up to 38 wt% MnO).

Most siliceous schists equilibrated under unusually high-f_{O_2} conditions that are inferred from common occurrences of braunite, ardennite and other highly oxidized phases (e.g., Enami 1986). The epidote minerals within the siliceous schists can be classified into three groups based on the atomic proportions in the octahedral M-sites (Fig. 7). One group is Mn- and Fe^{3+}-poor epidote with X_{Fe} = 0.11–0.21 and X_{Mn} < 0.01, that occurs in siliceous schists intercalated with pelitic schists. This group probably formed under low-f_{O_2} conditions. Another group most common in the siliceous schists, has compositions lying between X_{Fe} = 0.33 and X_{Mn} = 0.33 showing complete occupation of the M(3)-site with Fe^{3+} and Mn^{3+}. A third group is unusually poor in Al suggesting Fe^{3+} and Mn^{3+} incorporation into M(1) as well as M(3) (Enami and Banno 2001). This group characteristically contains significant amounts of Sr and Ba in A(2) and can be termed strontiopiemontite as will be described later (Table 2).

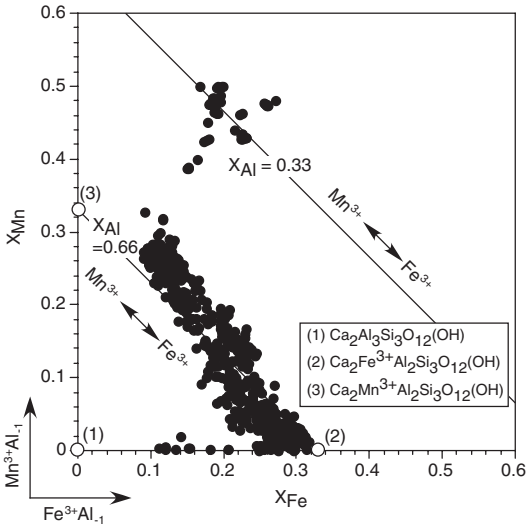

Figure 7. Compositional variations of epidote and piemontite of siliceous schists in the X_{Al}-X_{Fe}-X_{Mn} system (Enami and Banno 2001; Enami unpublished data).

Mafic schist. The typical mineral assemblage of mafic schist throughout the Sanbagawa belt is amphibole, chlorite, epidote, phengite, sodic plagioclase, and quartz. Amphibole compositions systematically change with increasing metamorphic grade from actinolite → winchite → crossite → barroisite → hornblende/pargasite under high-f_{O_2} conditions in which hematite is stable, and actinolite → hornblende/pargasite under low-f_{O_2} conditions. Pumpellyite occurs only in low-f_{O_2} mafic schists such as a pyrrhotite-bearing sample from the lower-grade part of the chlorite zone. Garnet becomes stable only in the albite- and oligoclase-biotite zones.

Epidote minerals in mafic schist are clinozoisite-epidote solid solutions (hereafter simply denoted as epidote) and have CaO > 20.4 wt% (> 1.78 pfu), MnO < 1.0 wt% and MgO < 0.9 wt%. The X_{Fe} value shows a wide range of 0.1 to 0.36 that is closely related to the composition

Table 2. Representative analyses of epidote minerals in the Sanbagawa metamorphic rocks.

Locality	Kotsu	Besshi		Asemi		Besshi			Tomisato		
Sample	0504	TOCP-01		AS582	M1	GE1501b		HU0311	GSJM31217		
Mineral	Ep	Zo	REE-Ep	Ep	Pie	Ep	Zo	Ep	Sr-Pie	Sr-Pie	Sr-Pie
SiO_2	36.7	39.5	35.60	36.5	37.1	38.1	39.4	38.3	31.1	30.0	31.1
TiO_2	0.11	0.10	n.d.	n.d.	0.00	0.00	0.08	0.15	0.48	0.27	0.53
Al_2O_3	21.6	32.5	24.55	20.9	18.8	25.5	31.4	28.6	8.92	6.25	8.95
Cr_2O_3	0.00	n.d.	n.d.	n.d.	n.d.	0.03	0.09	0.03	0.02	n.d.	n.d.
Fe_2O_3*	15.5	1.41	8.87	15.1	5.70	10.7	2.73	6.26	9.10	10.7	9.19
MnO	0.18	0.02	n.d.	0.70	14.9**	0.06	0.00	0.06	17.5**	18.7**	17.4**
MgO	0.00	0.02	n.d.	n.d.	0.05	0.22	0.04	0.03	0.02	0.01	0.01
PbO	n.d.	n.d.	n.d.	n.d.	n.d.	n.d.	n.d.	n.d.	5.44	7.55	5.61
SrO	2.24	n.d.	n.d.	2.83	0.13	1.11	0.14	0.14	8.59	9.98	8.68
BaO	n.d.	n.d.	n.d.	n.d.	n.d.	n.d.	n.d.	n.d.	6.44	3.66	6.71
CaO	21.0	24.7	16.05	21.0	22.0	22.4	24.0	23.0	10.2	10.1	10.3
Na_2O	0.01	0.00	n.d.	n.d.	0.00	n.d.	0.00	0.00	0.03	0.01	0.00
K_2O	0.00	0.00	n.d.	n.d.	0.00	n.d.	0.00	0.00	0.00	0.00	0.00
REE_2O_3	n.d.	n.d.	14.89†	n.d.	n.d.	n.d.	n.d.	n.d.	n.d.	n.d.	n.d.
Total	97.34	98.25	99.96	97.03	98.68	98.12	97.88	96.57	97.84	97.23	98.48
X_{Fe}§	0.31	0.03	0.19	0.31	0.11	0.21	0.05	0.12	0.22	0.27	0.23
Ref.	Eu	Eu	S84	Eu	Eu	Eu	Eu	Eu	EB01	EB01	EB01

* Total Fe as Fe_2O_3,
** Total Mn as Mn_2O_3, § $X_{Fe} = Fe^{3+}/(Al + Cr + Fe^{3+} + Mn^{3+})$.
† Includes La_2O_3 (3.21 wt%), Ce_2O_3 (7.05 wt%), Nd_2O_3 (1.55 wt%), Sm_2O_3 (1.70 wt%) and Gd_2O_3 (1.38 wt%).
Abbreviations for rock types are: Bs, mafic schist; Ps, pelitic schist; Ss, siliceous schist; KEc, kyanite-eclogite; EAm, epidote-amphibolite.
Other abbreviation: n.d., not determined.
References are: Eu, Enami (unpublished data); S84, Sakai et al. (1984); EB01, Enami and Banno (2001).

of associated opaque minerals. Epidote in pyrrhotite-bearing mafic schist mostly has X_{Fe} value of 0.10–0.22 whereas epidote that coexists with hematite typically has X_{Fe} value of 0.23–0.36 (Fig. 8). Stability of these two opaque minerals is strongly controlled by f_{O_2}; the occurrence of pyrrhotite indicates distinctly lower f_{O_2} than hematite-bearing assemblages (e.g., Itaya et al. 1985). Thus, the close relationship between the composition of epidote and coexisting opaque minerals clearly suggests that X_{Fe} is strongly controlled by f_{O_2} during metamorphism (see also Poli and Schmidt 2004, Grapes and Hoskin 2004). A more detailed inspection of the relationships between epidote composition and coexisting mineral paragenesis in terms of the Al-Ca-Fe^{3+} system with chlorite, albite, quartz, and H_2O-dominant fluid (Fig. 9; Nakajima 1982) indicates that under high-*P* pumpellyite-actinolite facies conditions the maximum and minimum X_{Fe} of epidote in mafic schist are defined by hematite + chlorite + sodic amphibole and pumpellyite + chlorite + actinolite, respectively.

Epidote-amphibolite and eclogite. Protoliths of these rock types are mainly mafic plutonic and volcanic rocks; some occur as layers within the metasediments (Banno et al. 1976a, b; Kunugiza et al. 1986; Takasu 1989). These rocks underwent extensive recrystallization under epidote-amphibolite facies conditions, and their typical mineral assemblages are similar to those of the surrounding mafic schists except for the common occurrence of garnet in the epidote-amphibolites. However, they also locally preserve evidence of a prior stage of eclogite facies metamorphism (e.g., Takasu 1989; Wallis and Aoya 2000). Most epidote minerals in epidote-amphibolite and eclogite (hereafter denoted as epidote-amphibolite) are clinozoisite-epidote with X_{Fe} = 0.07–0.27 (Fig. 10), CaO > 20.8 wt% (> 1.85 pfu), MnO < 0.7 wt% and MgO < 0.9 wt%. Zoisite occurs in an epidote-amphibolite derived from an inferred gabbroic protolith. Zoisite-rich layers (6 m in maximum thickness) intercalated with thin hornblende-rich layers (usually less than 1 m thick) occur in several epidote-amphibolite bodies (Banno et al. 1976a, b). The zoisite-rich rocks also contain subordinate amounts of kyanite, paragonite, phengite and quartz (Enami 1980), and are considered to have originally been cumulate anorthosite layers (Banno et al. 1976b; Yokoyama 1976). Zoisite has a limited compositional range of X_{Fe} = 0.02–0.05, CaO = 23.5–24.5 wt% (1.93–2.02 pfu), MnO < 0.08 wt% and MgO < 0.05 wt% (Fig. 10).

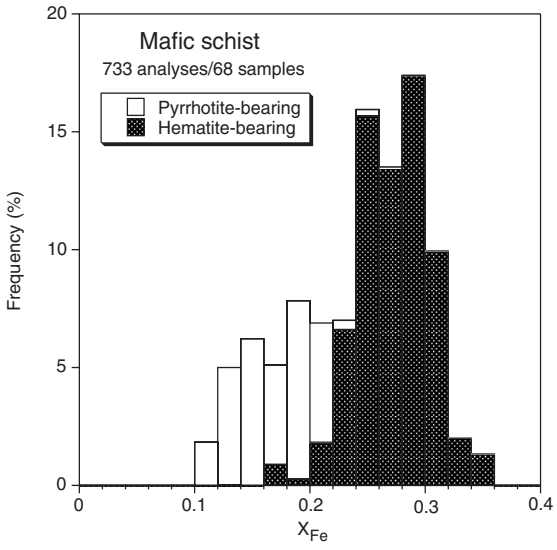

Figure 8. Frequency distribution of X_{Fe} of epidote in hematite- and pyrrhotite-bearing mafic schists from the Sanbagawa belt (Higashino et al. 1981; Higashino et al. 1984; Enami unpublished data).

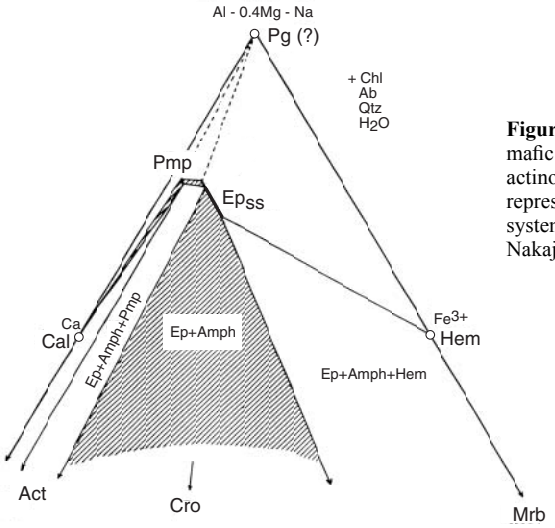

Figure 9. Paragenetic relations of mafic schists at HP pumpellyite-actinolite facies conditions graphically represented in the Al-Ca-Fe^{3+} ternary system (modified from Fig. 7 of Nakajima 1982).

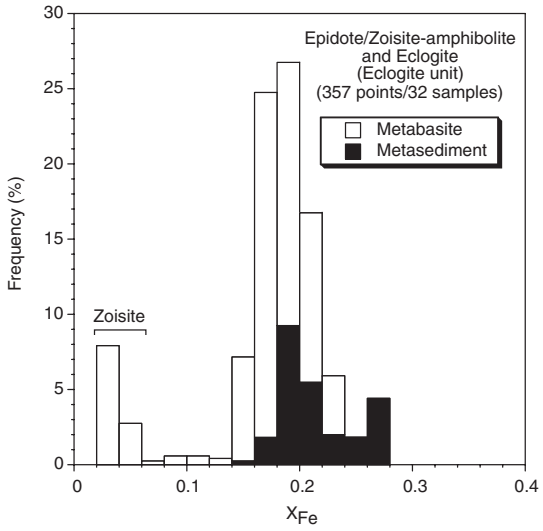

Figure 10. Frequency distribution of X_{Fe} of epidote and zoisite in metabasites and metasediments of the Sanbagawa eclogite unit (Enami, unpublished data).

Compositional change of epidote minerals with metamorphic grade

Epidote composition varies with temperature by (1) decreasing X_{Fe} and (2) enlargement of the compositional range towards lower X_{Fe} with increasing metamorphic grade. Coexisting epidote and pumpellyite in the mafic schists of the Sanbagawa belt were first documented by Nakajima et al. (1977) and Nakajima (1982). X_{Fe} of epidote coexisting with pumpellyite, actinolite, chlorite, albite, and quartz systematically decreases with increasing metamorphic grade (Fig. 11) and is controlled by the pumpellyite-consuming reaction (Fig. 12)

41 Pmp + 2 Chl + 47 Qtz = 71 Cz + 11 Act + 109 H_2O

A similar compositional change occurs in pelitic schists from the chlorite to garnet zone (Fig. 13). In this case, epidote is the only Ca-Al-silicate and the compositional shift cannot

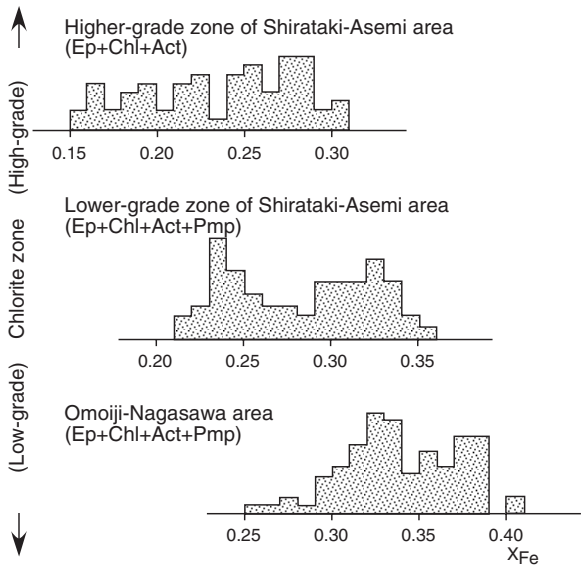

Figure 11. Frequency distribution of X_{Fe} of epidote in mafic schists of the HP pumpellyite-actinolite facies and lower-grade areas of the Sanbagawa belt (modified from Fig. 8 of Nakajima 1982).

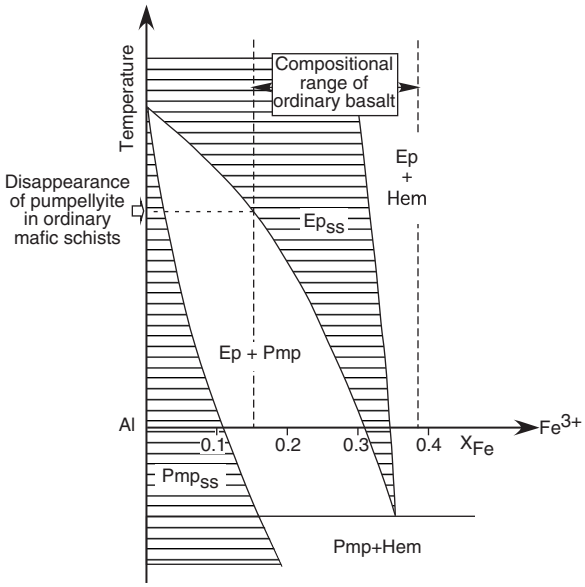

Figure 12. Al-Fe^{3+} pseudobinary phase diagram for the epidote-pumpellyite equilibrium (modified from Fig. 6 of Nakajima 1982).

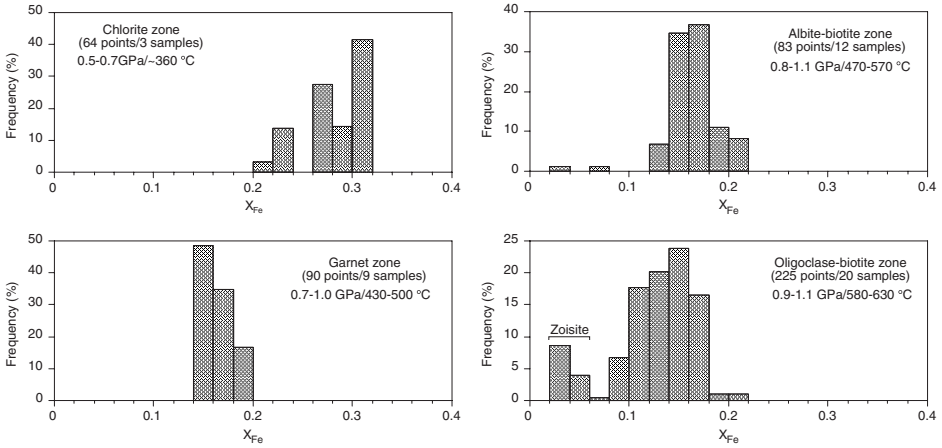

Figure 13. Frequency distribution of X_{Fe} of epidote in pelitic schists from the Sanbagawa belt (Higashino et al. 1981; Enami unpublished data).

be explained by a net transfer reaction. Poorly crystalline carbonaceous matter or disordered-graphite is common in pelitic schists of the chlorite zone instead of fully ordered graphite in garnet and higher-grade schist (Itaya 1981; Tagiri 1985). They might not have completely buffered f_{O_2} to reduced conditions, which may explain the high X_{Fe} of epidote in chlorite zone pelitic schists. The breakdown of detrital Ca-plagioclase in low-grade pelitic schists could possibly explain the decrease in epidote X_{Fe}. Goto et al. (2002) emphasized that calcite is common in the Sanbagawa pelitic schists and thus its occurrence has a significant role in mineral reactions. They proposed possible dehydration-decarbonation reactions to produce biotite and calcic amphibole, respectively, which are common in pelitic schists of the albite-biotite and oligoclase-biotite zones, as follows:

$$3\ Ms + 2\ Chl + 16\ Cal + 24\ Qtz = 3\ Bt + 8\ Cz + 12\ H_2O + 16\ CO_2, \quad \text{and}$$

$$4\ Chl + 9\ Ab + 22\ Cal + 13\ Qtz = 9\ Prg + 2\ Cz + 22\ H_2O + 22\ CO_2.$$

These reactions form clinozoisite as a high-*T* product, and can explain (1) increasing modal abundance of epidote with increasing metamorphic grade (Fig. 3 of Goto et al. 2002) and (2) support a general consensus that the zoning of epidote with decreasing X_{Fe} towards the margin is a prograde feature.

Enlargement of the epidote compositional field with increasing metamorphic grade has been documented by Miyashiro and Seki (1958) with optic axial angle measurements. They concluded that (1) X_{Fe} of epidote in pelitic and psammitic schists tends to be lower than that in mafic schist, and (2) the compositional range enlarges towards lower X_{Fe} with increasing metamorphic grade. These findings are confirmed by electron microprobe analyses of epidote (Fig. 13). The enlargement of the epidote compositional field and the presence of a two-phase loop between orthorhombic and monoclinic epidote minerals (Enami and Banno 1980) probably cause the appearance of zoisite in the albite-biotite and oligoclase-biotite zones (Figs. 10 and 13).

Studies on coexisting zoisite and epidote mainly in the Sanbagawa epidote-amphibolites and basic schists (Enami and Banno 1980) show that (1) clinozoisite contains distinctly higher X_{Fe} than coexisting zoisite suggesting the presence of a two-phase loop between zoisite and clinozoisite, (2) the compositional range of this two-phase loop shifts towards Fe^{3+}-rich

compositions with increasing metamorphic grade (Fig. 14), (3) zoisite solid solution, in relation to epidote solid solution, represents the higher *T* phase, and thus (4) the frequency of appearance of zoisite should increase with increasing metamorphic grade (Fig. 14; Table 2). Franz and Selverstone (1992) reported similar zoisite-clinozoisite phase relations and suggested that the clinozoisite-side limb of the loop shifts towards Fe^{3+}-rich compositions with increasing metamorphic pressure.

Single epidote grains commonly display zonal discontinuities that have been attributed to a compositional gap in the clinozoisite-epidote series with a crest composition at X_{Fe} = 0.17 to 0.20 (e.g., Strens 1965; Raith 1976). The compositional range of Sanbagawa epidotes, however, extends across the proposed compositional gap implying complete miscibility along the clinozoisite-epidote join under blueschist and high-*P* pumpellyite-actinolite facies conditions (cf. Grapes and Hoskins 2004).

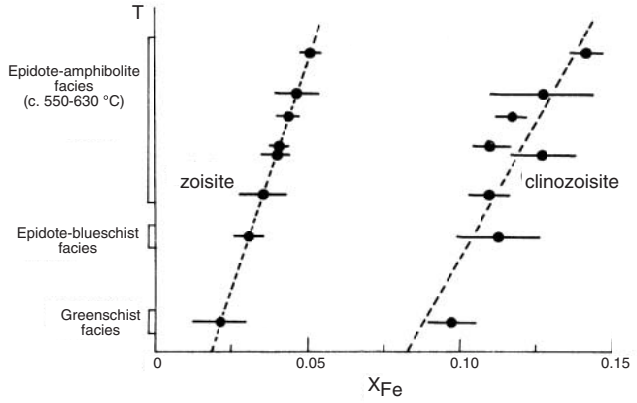

Figure 14. Relationship between X_{Fe} of coexisting zoisite and clinozoisite and metamorphic grade (modified from Fig. 5 of Enami and Banno 1980).

EPIDOTE MINERALS IN CALCAREOUS MEATASEDIMENTS OF THE ECLOGITE FACIES: EUROPEAN ALPS

Metacarbonates and calcareous metasediments are minor rock-types in HP metamorphic terranes that are closely related to the oceanic subduction system. The eclogite facies metasediments including impure marbles, siliceous dolomites, calc-mica schists and calc-schists are, however, widely distributed in the European Alps; these are rare lithological sequence in a HP terrane (e.g., Droop et al. 1990). Petrologic and mineralogical characteristics of the zoisite-bearing calcareous HP metasediments have been well documented from the Eclogite Zone of the Tauern Window, eastern Alps (Franz and Spear 1983; Spear and Franz 1986) and the Adula nappe, central Alps (Heinrich 1982). Many of the eclogite facies rocks are of early Alpine age of the Cretaceous. The eclogite facies event was followed by decompression and cooling to blueschist facies conditions.

Metamorphic conditions of the Eclogite Zone rocks in the Tauern Window during the high-*P* event have been estimated at 1.9–0.2 GPa/590–630°C (e.g., Hoscheck 2001). Typical eclogite facies assemblages include zoisite + dolomite + kyanite + quartz in kyanite marbles, zoisite + phengitic muscovite + dolomite + calcite + quartz in zoisite marbles (Fig. 15; Spear and Franz 1986), zoisite + diopside + tremolite + dolomite + calcite + quartz in siliceous dolomites (Franz and Spear 1983), and zoisite + dolomite + calcite + phengitic muscovite +

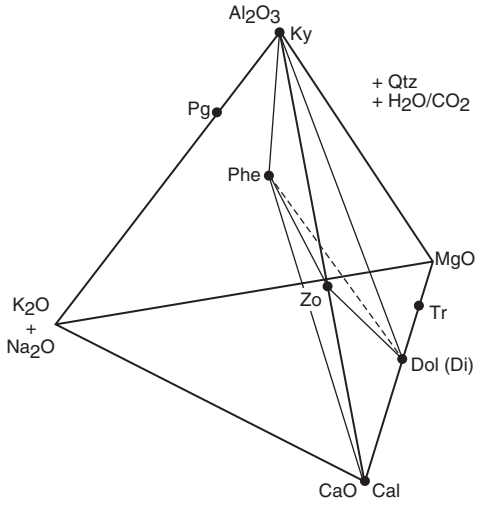

Figure 15. Phase relations of primary mineral assemblages in kyanite-zoisite marble from the Eclogite Zone, Tauern Window in the system Al_2O_3-CaO-MgO-(Na_2O, K_2O). Projection was made from quartz and a fluid phase of fixed H_2O/CO_2 (modified from Fig. 9 of Spear and Franz 1986).

garnet + quartz in calc-mica schists (Hoscheck 2001). Zoisite (X_{Fe} = 0.02–0.05) forms laths up to several mm in length, and is partly intergrown with garnet in the calc-mica schists. Zoisite in the zoisite marbles decomposed into paragonite, secondary muscovite, chlorite and kaolinite according to the following reactions:

$$Zo + Dol + Qtz + H_2O = Chl + Cal + CO_2,$$

$$Zo + Dol + NaCl/KCl + H_2O = Chl + Pg + Ms + CaCl_2 + CO_2, \quad \text{and}$$

$$Zo + HCl + H_2O = Kln + CaCl_2$$

(Spear and Franz 1986). In the calc-mica schists, clinozoisite/epidote occur as minor phases in the matrix (X_{Fe} = 0.15–0.17) and as inclusions in the garnet (X_{Fe} = 0.15–0.17).

Pressure and temperature conditions of the Adula nappe systematically increase from northern Vals area (1.0–1.3 GPa/450–550°C) through Confin-Trescolmen area (1.2–2.2 GPa/450–550°C) to southern Gagnone-Arami-Duria area (1.5–3.5 GPa/600–900°C) (Heinrich 1982, Droop et al. 1990). The zoisite-bearing calc-schists occur in the central and northern areas, and include assemblages of zoisite + dolomite + garnet + omphacite + kyanite + quartz, zoisite + dolomite + garnet + omphacite + quartz + hornblende + phengite + paragonite, and zoisite + calcite + garnet + phengite + quartz (Heinrich 1982).

PARAGENESIS OF EPIDOTE MINERALS IN HP TO UHP ROCKS

The generalized *P-T* path of HP to UHP rocks shows at least four discrete stages of metamorphic crystallization: (I) the prograde stage during subduction from (sub)greenschist to blueschist, epidote-amphibolite, and even eclogite facies conditions, (II) the peak stage from blueschist or epidote-amphibolite to various eclogite facies conditions, even up to depths otherwise typical for the Earth's mantle, (III) a first retrograde epidote-amphibolite or amphibolite facies overprint during exhumation to crustal depths of < 35 km, and (IV) a second retrograde greenschist facies overprint during final uplift. Such a four-stage metamorphic evolution is exemplified by kyanite-bearing and kyanite-absent eclogites of the western Dabie (Fig. 16; Eide and Liou 2000). The prograde assemblage (stage I) of these eclogites comprises amphibole, epidote (X_{Fe} = 0.21–0.28), phengite, quartz, and rutile, all occurring as inclusions

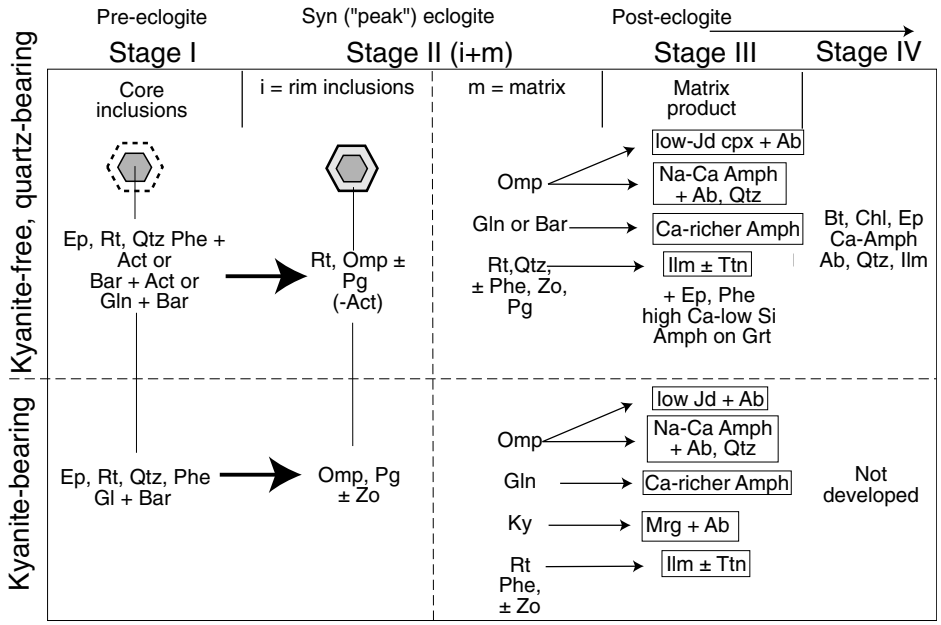

Figure 16. Four-stage metamorphic evolution of kyanite-bearing and kyanite-absent eclogites from the Dabie terrane showing the occurrence of epidote/zoisite in 4 different stages of HP and UHP metamorphism (see text for explanation). The two eclogite types in the rows are respectively UHP kyanite-bearing eclogite and HP quartz-bearing kyanite-free eclogite from western Dabie (modified from Fig. 4 of Eide and Liou 2000).

in garnet. The eclogite facies peak assemblage (stage II) consists of garnet, omphacite, rutile, amphibolite, coesite/quartz, and/or kyanite and ± phengite, zoisite (X_{Fe} = 0.03–0.07), and paragonite. The stage II assemblage can be further subdivided into IIi and IIm, distinguished on textural grounds by eclogite facies inclusions in garnet rims (IIi) and by matrix minerals (IIm). In stage III, titanite (± ilmenite) replaces rutile and epidote (X_{Fe} = 0.21 ± 0.05) and Ca-amphibole replace garnet. Stage IV of upper greenschist facies conditions includes epidote (X_{Fe} = 0.31–0.33), albite, quartz, and titanite or biotite + chlorite pseudomorphs after garnet. This example underlines the importance of epidote minerals for the study of HP to UHP rocks. Due to their wide *P-T* stability field and occurrence in a variety of bulk rock compositions, epidote minerals could form during each of the four stages normally encountered by these rocks. They typically occur from small inclusions (< 50 μm) to large porphyroblasts (up to 2 mm) in the pre-, syn- and post-peak metamorphic assemblages of coesite-bearing eclogites and associated rocks. Because of the well known sluggish reaction kinetics of epidote minerals, it is likely that once they have formed they might persist metastably without re-equilibration, such that their chemical zoning in major and trace elements records the complex *P-T* history of these rocks.

The prograde evolution of HP to UHP rocks

During the prograde stage, the protoliths of UHP rocks may have passed through (sub) greenschist, greenschist, blueschist, and/or epidote-amphibolite facies and developed the typical successions of mineral paragenesis described above for subduction zone metamorphism. All protoliths of UHP rocks, however, pass and probably recrystallize under quartz-eclogite facies conditions before entering the UHP domain. In mafic rocks the prograde quartz-eclogite

facies recrystallization results in a combination of garnet, katophoritic amphibole, paragonite, omphacite, rutile, and epidote minerals. The prograde phases of HP to UHP rocks typically occur as inclusions in garnet porphyroblasts but also in omphacite, and/or kyanite. These inclusions are abundant in quartz eclogite but are comparatively rare in coesite eclogite. Enami et al. (1993) and Zhang et al. (1995a) used such prograde inclusions in garnet together with the garnet core compositions to constrain the prograde *P-T* path of the Donghai UHP eclogite through epidote-amphibolite and quartz eclogite facies conditions. One very prominent texture of the prograde evolution of UHP rocks is found in coronitic meta-granitoids and metagabbros in which primary magmatic minerals, especially plagioclase, are pseudomorphically replaced by typical HP mineral paragenesis including zoisite (Fig. 17). Well-preserved igneous textures and pseudomorphs after original magmatic phases are described in the UHP meta-granitoids of the Brossaco-Isasca unit of the Dora-Maira Massif (western Alps; Bruno et al. 2001) and the Sulu terrane of eastern China (Hirajima et al. 1993). In these rocks, magmatic plagioclase is replaced by zoisite, jadeite, quartz, K-feldspar, and kyanite and various coronitic reactions developed between biotite and adjacent minerals. Zoisite occurs as needle-like crystals < 10 μm long, jadeite as stumpy crystals from 5 to 20 μm across and kyanite as prismatic crystals of variable size included in amoeboid patches of K-feldspar ($Or_{90}Ab_{10}$). Zoisite and kyanite are pure, sodic pyroxene is a solid solution of jadeite, Ca-Tschermak and Ca-Eskola. A pseudomorphic reaction is

$$4\ \mathrm{Pl} + x\ \mathrm{H_2O} = 2x\ \mathrm{Zo} + x\ \mathrm{Ky} + (x{+}4y)\ \mathrm{Qtz} + 4y\ \mathrm{Jd} + (4 - 4x - 4y)\ \mathrm{Kfs}$$

where x and y are the molar proportions of anorthite and albite, respectively in a plagioclase of composition $(Ca_xNa_yK_{1-x-y})(Al_{1+x}Si_{1-x})Si_2O_8$ (Bruno et al. 2001). Zhang and Liou (1997a) describe the preserved prograde gradational sequence from incipiently metamorphosed gabbro (referred to as coronitic metagabbro) over partly to strongly recrystallized gabbro (referred to as transitional metagabbro) to completely recrystallized coesite eclogite within a single boulder (about 30 m in diameter) from Sulu. This boulder was found adjacent to the above-mentioned

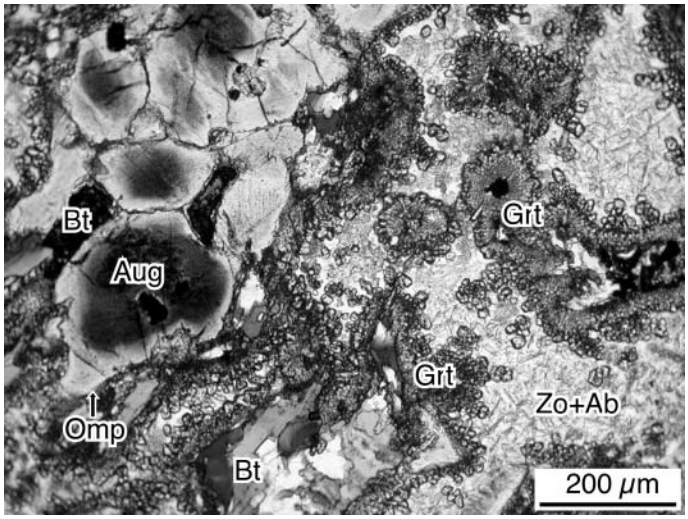

Figure 17. Photomicrograph (open nicol) of a meta-granitoid from Yangkou of the Sulu UHP terrane (Enami unpublished). Igneous augite with tiny inclusion of Fe-oxides is partly rimmed by very thin omphacite. Coronitic garnet is developed between igneous biotite and plagioclase that is pseudomorphed by fine aggregates of zoisite and albite. Biotite is partly replaced by aggregates of Ti-rich phengite (cf. Hirajima et al. 1993).

meta-granitoid described by Hirajima et al. (1993). The coronitic metagabbro preserved relict gabbroic texture and minerals. Primary plagioclase broke down to zoisite, albite, kyanite, phengite, and ± amphibole. In the transitional metagabbro, augite and orthopyroxene are totally replaced by omphacite, and the lower-*P* assemblage zoisite, albite, kyanite, phengite, and garnet coexists with domains of omphacite, kyanite, and phengite in pseudomorphs after plagioclase. The coesite eclogite contains the typical UHP assemblage omphacite, kyanite, garnet, phengite, coesite/quartz, and rutile but still preserve a faint gabbroic texture. Estimated *P-T* conditions for the different prograde stages recorded in this unique rock are 540 ± 50°C at ~1.3 GPa for the coronal stage, 600-800°C at ≥ 1.5–2.5 GPa for the transitional stage and 800-850°C at >3.0 GPa for the UHP peak metamorphism.

A nearly monomineralic epidosite was suggested to be the parent rock for an UHP grossular-rich garnetite boudin that contains ~80 vol% garnet ($Grs_{63}Alm_{25}Prp_7And_4$; 0.10–0.18 wt% Na_2O) and 15 vol% hercynite + anorthite symplectite after kyanite in migmatitic gneiss of the Gföhl unit in the easternmost Moldanubian Zone, the Bohemian Massif (Vrána and Gryda 2003). This suggestion was based on nearly identical major composition of epidote (X_{Fe} = 0.23–0.48) to grossular-rich garnetite and supported by about 4 times higher whole-rock REE abundances than those in Moldanubian paragneisses. Moreover, epidosite occurs in some 'stratiform' garnet-pyroxene Ca-Fe-Mg skarns in the Moldanubian Zone. In the process of epidotization, epidote would scavenge REE from fluids or surrounding rocks, due to the isomorphism in the series epidote-allanite. Although the index mineral coesite was not found, the elevated Na content in the garnet provides independent evidence of the UHP history of the rock. An approximate *P-T* estimate yields pressure ≈ 4 GPa, *T* of 970–1100°C. A reaction based on the paragenesis and composition of garnetite is

$$0.37\ Ttn + 6\ Ep\ (X_{Fe} = 0.25) + Mag + 1.25SiO_2 = 4.25\ Grs + 2.50\ Alm + 0.75\ Rt + 3H_2O + 1.37O_2$$

The peak metamorphism of HP to UHP rocks

Only those epidote minerals that contain inclusions of coesite and/or coesite pseudomorphs can be unequivocally considered stable at UHP conditions. Nevertheless, previous descriptions often also list zoisite or clinozoisite in the peak UHP assemblage based on petrographic observation and experimental studies. Zoisite (with X_{Fe} below 0.05) is a common phase in HP and UHP rocks as it is known to be stable up to almost 7 GPa and ≈ 1000°C (Poli and Schmidt 2004). It coexists with garnet and omphacite in many zoisite-kyanite eclogites and even in coesite-bearing eclogites. Yao et al. (2000) describe coesite inclusions in zoisite from different mineral assemblages (in estimated vol%) within a banded eclogite from northern Sulu:

(a) normal eclogite (30-60 % Grt, 20–50% Omp, 2–10% Qtz, 0–5% Ky, 0–5% Zo, 1–2% Rt, and <2% carbonate)

(b) garnet-rich eclogite (60–90% Grt, 5–20% Qtz, 5–15% Omp, 0–2% Zo, 0–5% Ky, 0 –5% Phe, and 2–5% Rt)

(c) zoisite- and kyanite-rich eclogite (20–70% Zo, 20–35% Ky, >10% Qtz, > 10% Phe, with minor Grt, Omp, and Rt)

(d) leucocratic thin layer (> 50% Qtz, 5–10% Ky, 10–15% Zo, 5–10% Phe, 20–30% Pl, with minor Grt, Cpx, Amph, and Rt)

This example illustrates the stable coexistence of zoisite with coesite and kyanite. This assemblage is common to most HP and UHP terranes and results from the breakdown of plagioclase (i.e., in its simplest form, $An + H_2O = Zo + Ky + Coe/Qtz$; Newton and Kennedy 1963).

Compared to zoisite, epidote (typically with X_{Fe} > 0.14) is less common in eclogite

facies rocks. The maximum *P*-limit of epidote is not well defined. However, Zhang (1992) first reported inclusions of pseudomorphs of fine-grained quartz aggregates after coesite in a euhedral epidote crystal (Figs. 18A and B) with X_{Fe} = 0.23 from Sulu and suggested that epidote was stable together with coesite, garnet, and omphacite at about 850°C and 3.2 GPa. Inclusions of coesite pseudomorphs in epidote were then described by Hirajima et al. (1992) in nyböite eclogite in Donghai of the southern Sulu belt and recently in Himalayan coesite-bearing eclogite by Massonne and O'Brien (2003). These findings established the stability of epidote at UHP conditions. Since the first description of Zhang (1992), other localities with comparable inclusions of coesite in epidote minerals have been recognized.

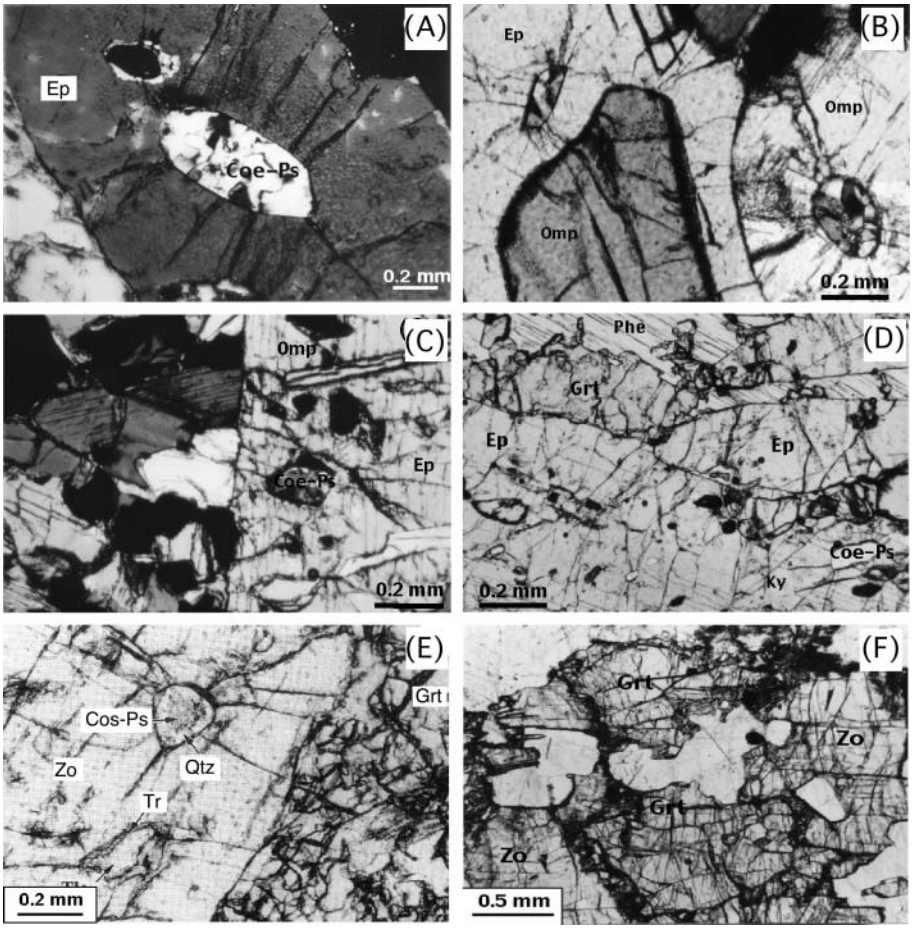

Figure 18. Photomicrographs of UHP epidote and zoisite from the Dabie-Sulu and Kokchetav terranes. (A) Porphyroblastic epidote with inclusions of coesite-pseudomorphs in eclogites from Sulu (after Zhang et al. 1995a), (B) Coesite-pseudomorphs in epidote and omphacite from Qinglongshan eclogite (A and B crossed polarized light; Zhang R. unpublished), (C) Porphyroblastic epidote with inclusions of omphacite, garnet, kyanite and coesite-pseudomorph cross-cut the foliation defined by alignment of kyanite, omphacite and talc in Qinglongshan eclogite (C to F plain polarized light; after Zhang et al. 1995a), (D) Coesite-pseudomorph in epidote from foliated Qinglongshan eclogite (Zhang R. unpublished), (E) Coesite inclusions in zoisite of Bixiling talc-kyanite eclogite (after Zhang et al. 1995b), (F) Coarse-grained zoisite in equilibrium with diamond-bearing garnet from Kokchetav gneiss (Zhang R. unpublished).

Epidote and zoisite with inclusions of coesite or coesite pseudomorphs in Dabie-Sulu. Inclusions of coesite or coesite pseudomorphs in epidote and zoisite have been described from several Dabie-Sulu eclogites (Zhang 1992; Hirajima et al. 1992; Zhang and Liou 1994; Zhang et al. 1995a; Rolfo et al. 2000; Yao et al. 2000). Most of these eclogites contain kyanite ± talc in addition to the common assemblage of garnet, omphacite, rutile, and coesite/quartz. Inclusions of coesite are exclusively described in zoisite whereas epidote contains only inclusions of coesite pseudomorphs.

The Bixiling metamorphic complex is the largest UHP body in Dabie. It consists of different types of eclogites that contain thin layers of garnet-bearing cumulate ultramafic rocks. Differences in the bulk composition result in a distinct layering of some of the eclogitic rocks defined by different mineral assemblages and extent of retrograde recrystallization. These layered eclogites range in thickness from about 2 to 10 m and grade from (a) beige-colored kyanite-rich eclogite, (b) kyanite-bearing eclogite that contains minor zoisite and talc through (c) dark brown barroisite-bearing eclogite to (d) rutile-rich brown eclogite. In the type (b) kyanite-bearing eclogite zoisite belongs to the peak stage assemblage whereas epidote is a retrograde phase in both the barroisite-bearing and rutile-rich Fe-Ti eclogites. The coherent layering of the eclogitic rocks suggests a cumulate origin with anorthositic plagioclase to olivine-rich gabbro cumulate as the protolith. Eclogite facies metamorphism of these layered gabbros occurred at 610–700°C and $P > 2.7$ GPa, whereas amphibolite-facies retrograde metamorphism is characterized by symplectite of plagioclase and hornblende after omphacite and replacement of tremolite after talc at $P < 0.6$–1.5 GPa and $T < 600$°C.

Beside the layered eclogites, a zoisite-rich talc-bearing coesite eclogite occurs in Bixiling. This eclogite is composed of zoisite (20–50 vol%), garnet, omphacite, coesite/quartz, talc, ± kyanite, and minor rutile and phengite and low in Fe and Ti contents. Zoisite ($X_{Fe} \sim 0.03$) forms prismatic crystals up to 5 mm long and contains inclusions of coesite and coesite pseudomorphs with well-developed radial fractures (Fig. 18E).

The variation in paragenesis and composition of minerals as a function of bulk composition for the zoisite-bearing eclogite assemblages of Bixiling can be best discussed in the Al_2O_3-MgO-FeO-CaO tetrahedron projected from H_2O, SiO_2, jadeite, and rutile (Zhang et al. 1995b). To delineate the Fe/Mg ratio for garnet and omphacite for eclogite assemblages, the composition of these phases is projected from zoisite onto the AFM triangle (Fig. 19). In this projection, the position of garnet depends on the amount of grossular component and the Mg/(Mg + Fe) ratio. Eclogitic garnet with high grossular content has low $(Al_2O_3 - 0.75CaO)/[(Al_2O_3 - 0.75CaO) + MgO + FeO]$ and a high Mg/(Mg + Fe) ratio. Garnet of zoisite-talc-rich eclogites contains a very high grossular component (35 to 40%) compared to garnet from the other eclogites (18 to 26 %). Omphacite plots at negative co-ordinates, the extent depending on the amount of the jadeite component.

Several features are apparent from Fig. 19: (1) eclogitic assemblages show a systematic distribution of tie-lies among coexisting phases; (2) tie lines for eclogitic garnet - clinopyroxene systematically shift from Fe-Ti rich to the Mg-Al rich samples and are nearly parallel to one another. Garnet in the Fe-Ti rich layers is higher in the almandine component, and coexisting clinopyroxene contains higher Fe than counterparts in the Mg-Al rich layers. Garnet coexisting with talc and zoisite has a higher grossular content than garnet with kyanite + talc. The systematic disposition of these tie-lines suggests that they are equilibrium assemblages. Mafic rocks must have either high Mg content or high f_{O_2} in order to stabilize talc in the coesite stability field (see below). In the Donghai area of southern Sulu, several different HP to UHP eclogites and associated gneiss and quartzite contain trace to moderate amounts of either epidote or zoisite (e.g., Hirajima et al. 1992; Zhang et al. 1995a; Zhang et al. 2003):

- In a banded nyböite-bearing eclogite epidote occurs together with variable amounts of garnet, clinopyroxene, kyanite, phengite, Al-rich titanite, rutile, apatite, and quartz

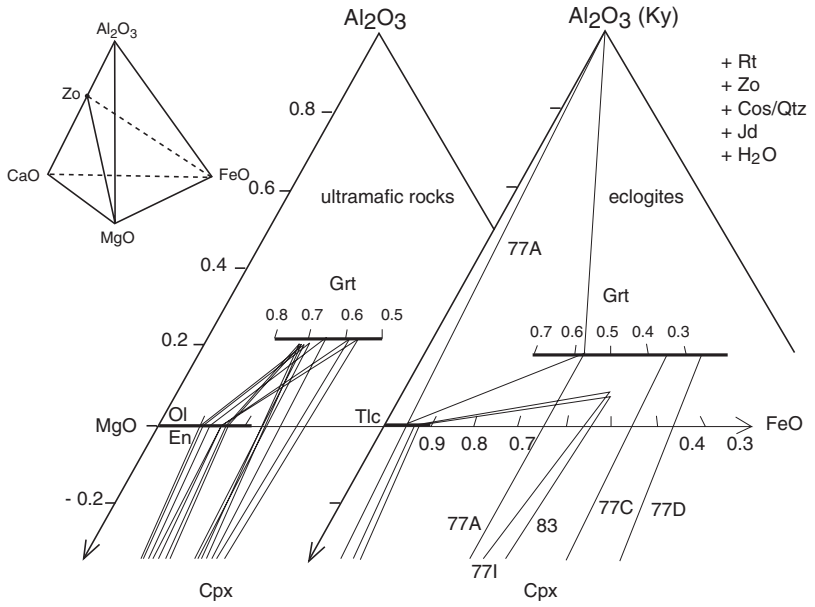

Figure 19. AFM diagram showing paragenesis and Fe-Mg partitioning between garnet and clinopyroxene from mafic-ultramafic layers of various compositions at nearly consistent *P-T* conditions. The AFM diagram is a projection from zoisite of the phase relations in the ACFM diagram. Sample numbers refer to eclogites of different compositions; some contain talc and kyanite as UHP assemblage in addition to garnet + omphacite + rutile + coesite. Garnets from both mafic-ultramafic layers are also grossular rich. For details see text (modified from Fig. 8 of Zhang et al. 1995b).

pseudomorphs after coesite. This eclogite was formed at about 740 ± 60°C and P > 2.8 GPa. Epidote commonly has allanitic cores with several wt% of REE. In an epidote porphyroblast-rich band inclusions of polycrystalline quartz aggregates after coesite are found in epidote with X_{Fe} = 0.24 (Figs. 18A–D).

- Epidote eclogites display the representative assemblage of garnet, omphacite, kyanite, coesite/quartz, rutile, epidote, ± phengite and barroisite and are characterized by >5 vol% porphyroblastic epidote. They are foliated and exhibit two stages of equilibration within the coesite stability field. The earlier stage consists of medium-grained garnet, omphacite, kyanite, epidote, and rutile that define the rock foliation. The second stage resulted in the formation of coarse-grained epidote ± barroisite porphyroblasts that cut the foliation and contain inclusions of earlier minerals. Both medium-grained eclogitic minerals and porphyroblastic epidote contain inclusions of quartz pseudomorphs after coesite with well-developed radial fractures. A quartz-rich, massive variety of the epidote eclogites contains abundant inclusions of pre-eclogite stage minerals such as paragonite, amphibole, albite, and rare aggregates of paragonite, barroisite, magnesite, and zoisite in garnet.
- Mattinson et al. (in review) differentiated several stages of epidote from epidote-rich talc-kyanite-phengite eclogites from Qinglongshan. Epidote I occurs as inclusion in garnet and later epidote; large epidote poikiloblast II, which enclose garnet, omphacite, epidote I, quartz (including coesite pseudomorphs); epidote III with a vermicular intergrowth of optically continuous quartz but lacking coesite

pseudomorphs; and retrograde rims in extensively amphibolitized samples (Ep IV). Some of the epidote grains are aligned with the foliation defined by omphacite and phengite, but most poikiloblasts cross cut it. Analyses of the various epidote types (Table 3, Fig. 20) show that poikiloblasts of Ep II and Ep III in fresh eclogites contain X_{Fe} = 0.15 to 0.18; the composition is similar in different samples, though one epidote lath which contains talc and phengite inclusions has an Fe-poorer medial zone suggesting incomplete replacement of low-Fe epidote by high-Fe epidote. Prograde Ep I and retrograde Ep IV grains contain up to X_{Fe} = 0.26. Skeletal epidote in gneiss and quartzite is zoned with X_{Fe} = 0.13 cores surrounded by thin rims of X_{Fe} = 0.31 and up to 1 wt% MnO.

- Zoisite-rich kyanite eclogite contains >5 vol% kyanite and locally up to 30 vol% zoisite instead of epidote. Some foliated eclogites are defined by elongated coarse-grained zoisite and omphacite, and fine-grained kyanite, garnet and rutile; coarse-grained zoisite porphyroblasts have grown across the foliation. Inclusions of quartz pseudomorphs after coesite occur in omphacite. Multi-mineral inclusions of garnet, hornblende, zoisite and Mg-chlorite occur in coarse-grained garnet.
- Talc-bearing eclogite consists of abundant kyanite and zoisite/clinozoisite or epidote, and contains polycrystalline quartz inclusions within eclogitic minerals. In Qinglongshan, it contains porphyroblastic euhedral epidote (2–10 mm) in a foliated fine-grained matrix of garnet, omphacite, kyanite, epidote (0.5–3 mm), quartz, and rutile. Porphyroblastic epidote-zoisite (c. 5 vol%) developed within and across the foliation contains numerous inclusions of eclogite facies minerals and polycrystalline quartz aggregates after coesite.

Kyanite quartzite occurs as thin layers (type I) with eclogite or as a country rock (type II) of eclogite pods. Massive kyanite quartzite of type II consists of 70 vol% quartz, 12 vol% epidote, 13 vol% kyanite + omphacite, 3 vol% garnet, 2 vol% phengite, and minor rutile. Epidote aggregates are locally abundant and contain coesite pseudomorphs as inclusions. Foliated kyanite quartzite of type I contain similar assemblages but lacks omphacite. Kyanite occurs either as euhedral coarse-grained discrete crystals or as fine-grained inclusions in phengite and epidote. Phengite and kyanite are mantled by a thin (0.02–0.05 mm) corona of biotite, and white mica (inner) + albite (outer), respectively. Inclusions of polycrystalline quartz aggregates occur in kyanite and epidote.

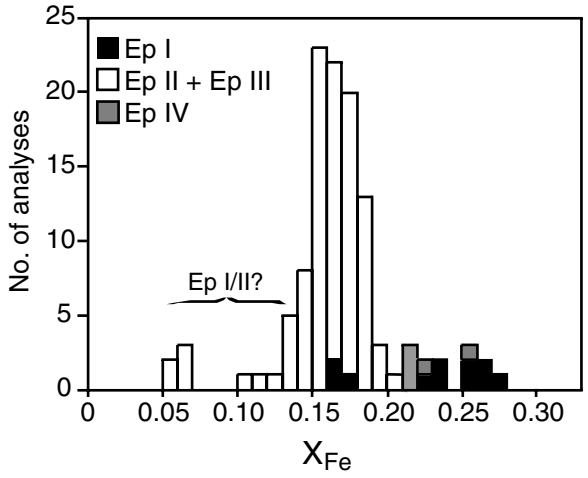

Figure 20. Frequency distribution of X_{Fe} of epidote in eclogites from Qinglongshan, Su-lu terrane Most epidote poikiloblasts (Ep II + Ep III) have X_{Fe} = 0.15 to 0.18; The Fe-poor medial region of a grain (Ep I) with prograde inclusions contains the lowest analyzed X_{Fe}; the Fe-richer core and rim of this grain are similar to the poikiloblast compositions. Fe-rich (X_{Fe} = 0.20–0.26) analyses include both prograde (Ep I) and late retrograde (Ep IV) grains (Mattinson et al. in review).

Table 3. Representative analyses of epidote minerals from Dabie, Sulu and Kokchetav terranes.

Terrane	Dabie						Sulu				
Locality	Bixiling		Shuanghe				Qinglongshan				
Rock Type	ZEc	ZEc	CEc	EEc	GBG	OG	TEc	Ec	Ec	Ec	KQz
Sample	77I	77I	CD29	CD36	92H22	SH6-1	SL-25F	QL1C-r	QL3-i	QL32-r	SL25
Mineral	Zo (r)	Zo (c)	Ep	Ep	Ep	Ep	Ep	Ep	Ep	Ep	Ep
SiO_2	39.38	39.31	39.97	38.68	38.62	38.83	37.86	37.64	37.56	38.43	37.55
TiO_2	0.04	0.04	0.08	0.09	0.09	0.11	0.30	0.14	n.d.	n.d.	0.13
Al_2O_3	31.82	32.35	27.11	25.57	25.83	27.93	24.50	23.79	24.31	26.77	25.18
Cr_2O3	0.03	0.05	0.34	0.03	0.02	0.03	n.d.	n.d.	n.d.	n.d.	0.00
Fe_2O_3*	1.79	1.33	7.34	10.13	10.02	6.68	13.35	13.80	13.12	9.46	11.96
MnO	0.02	0.00	0.07	0.23	0.17	0.11	0.01	0.16	0.16	0.07	0.04
MgO	0.02	0.01	0.16	0.03	0.04	0.00	0.37	0.10	0.20	0.22	0.21
SrO	n.d.	n.d.	n.d.	n.d	n.d.	n.d.	n.d.	n.d.	n.d.	n.d.	n.d.
CaO	24.29	23.55	22.31	23.96	23.01	24.41	22.43	22.94	22.04	23.17	21.90
Na_2O	0.00	0.00	0.15	0.00	0.02	0.01	0.02	n.d.	n.d.	n.d.	0.00
K_2O	0.00	0.00	0.09	0.01	0.01	0.00	0.01	n.d.	n.d.	n.d.	0.00
Total	97.39	96.64	97.62	98.73	97.83	98.11	98.85	98.57	97.39	98.12	96.97
X_{Fe}**	0.03	0.03	0.15	0.20	0.20	0.13	0.26	0.27	0.26	0.18	0.23
Ref.	Z95b	Z95b	C95	C95	C95	C95	Z95a	M	M	M	Z95a

Table 3. *continued on following page*

Table 3. *continued from previous page*

Terrane	Sulu								Kokchetav		
Locality	Caihu		JC	CZ	MZ	HT	YK	WH			
Rock Type	Ec	Ec	SEc	ZEc	ZEc	KQz	MGa	CSr	GZG	Ec	Ws
Sample	91CH08b		88J5	88C2	87D2	HZ9	YK3	91-6E	K8-41	K26	K21
Mineral	Zo	Ep	Ep	Zo	Zo	Zo	Zo*	Zo	Zo	Ep (i)	Zo (i)
SiO_2	38.4	37.6	38.39	39.52	39.73	38.45	39.94	39.40	39.57	37.54	39.59
TiO_2	0.11	0.06	n.d.	n.d.	n.d.	0.08	0.03	0.00	0.01	0.08	0.03
Al_2O_3	31.1	28.4	24.66	32.12	32.29	31.58	32.54	32.72	33.13	26.44	33.48
Cr_2O_3	0.20	0.04	n.d.	n.d.	n.d.	n.d.	0.02	0.04	0.01	0.05	0.42
Fe_2O_3*	2.14	5.09	13.56	1.41	2.04	1.89	1.62	0.22	1.03	8.57	1.19
MnO	0.03	0.04	n.d.	n.d.	n.d.	n.d.	0.01	0.01	0.07	n.d	0.07
MgO	0.00	0.14	0.26	0.44	0.00	0.04	0.04	0.02	0.15	0.04	0.03
SrO	1.20	2.66	n.d.	n.d.	n.d.	n.d	n.d.	n.d.	n.d.	n.d.	n.d.
CaO	23.1	22.0	22.29	23.85	24.09	23.38	23.61	24.31	24.45	23.25	24.44
Na_2O	n.d.	n.d.	n.d.	0.00	0.00	n.d.	0.50	0.00	0.01	0.03	0.02
K_2O	n.d.	n.d.	n.d.	n.d.	n.d.	n.d.	0.04	0.02	0.00	0.11	0.00
Total	96.50†	96.03	99.16	97.34	98.15	95.42	98.35	96.74	98.43	96.11	99.27
X_{Fe}**	0.04	0.10	0.26	0.03	0.04	0.04	0.03	0.00	0.02	0.17	0.02
Ref.	NE98	NE98	Z95a	Z95a	Z95a	Z95a	ZL97	Z95c	Z97	Z97	Z97

* Total Fe as Fe_2O_3 ** $X_{Fe} = Fe^{3+}/(Al + Cr + Fe^{3+} + Mn^{3+})$

† Includes Ce_2O_3 (0.14 wt%) and Nd_2O_3 (0.08 wt%) n.d. = not determined

Abbreviations for rock-types: ZEc, zoisite eclogite; CEc, carbonate eclogite; EEc, epidote eclogite; CBG, garnet-biotite gneiss; OG, orthogneiss, TEc, Talc eclogite; Ec, eclogite; KQtz, kyanite quartzite; SEc, Al-titanite eclogite; MGa, metagabbro; CSr, calc-silicate rock; GZG, Grt-Zo gneiss; Ws, whiteschist.

Abbreviations for localities: JC, Jianchang; CZ, Chizhuang; MZ, Mengzhuang; HT, Hetang; YK, Yangko; WH, Weihai.

References: Z95b, Zhang et al. (1995b); C95, Cong et al. (1995), Z95a, Zhang et al. (1995a); M, Mattinson et al. (in press); NE98, Nagasaki and Enami (1998); ZL97, Zhang and Liou (1997); Z95c, Zhang et al. (1995c); Z97, Zhang et al. (1997).

Microprobe analyses show no significant difference in the X_{Fe} value between epidote inclusions (X_{Fe} = 0.19–0.24) and porphyroblastic epidote (X_{Fe} = 0.18–0.25). A few porphyroblastic epidotes display compositional zoning with a slight decrease from cores of X_{Fe} = 0.25 to rims of X_{Fe} = 0.22. Epidote from kyanite quartzite has an X_{Fe} value of 0.23. Only a few eclogitic zoisites have been analyzed; their X_{Fe} values range from 0.03 to 0.04. Zoisite in kyanite quartzite has X_{Fe} value of 0.04. Clinozoisite of garnet-quartz-jadeite rocks ranges from X_{Fe} = 0.10–0.14.

Epidote minerals in Kokchetav diamond-bearing gneiss. Microdiamond inclusions are mainly restricted to garnet, clinopyroxene, and zircon from felsic gneiss, marble and garnet-clinopyroxene rocks. Zhang et al. (1997, 2002) reports garnet-zoisite gneiss with quartz, plagioclase, potassium feldspars (50 vol%), garnet (25 vol%), zoisite (5 vol%), and tourmaline (5 vol%) in addition to minor biotite, chlorite, opaque, apatite, and zircon (Table 3). Garnet contains abundant inclusions of diamond; idioblastic and porphyroblastic zoisite crystals are in sharp contact with porphyroblastic diamond-bearing garnet (Fig. 18F) suggesting that zoisite is stable with garnet in the stability field of diamond. The associated eclogites exhibit the common assemblage garnet, omphacite, rutile, coesite/quartz, ±zoisite and kyanite. Inclusions of quartz pseudomorphs after coesite were identified in 2 to 3 mm large garnet. Zoisite-rich eclogite displays abundant S-shaped inclusion trails of minute titanite crystals in the core and zoisite ± quartz in the rim of garnet.

Diamond-bearing clinozoisite gneiss at the western extremity of the Kokchetav massif (Korsakov et al. 2002) contains mainly retrograde phases including quartz (10–60 vol%), biotite (10–40 vol%), garnet (5–30 vol%), clinozoisite (5–20 vol%), clinopyroxene (0–15 vol%) and K-feldspar (5–10 vol%) with minor kyanite, amphibole, chlorite, calcite, tourmaline, and zircon, rutile, titanite, apatite, graphite as accessory minerals. Diamond, coesite, and other UHP minerals formed at 950–1000°C and >4.0 GPa are preserved only as inclusions in garnet, kyanite, and zircon. Bulk rock composition suggests that they are metamorphosed Ca-rich clays. Clinozoisite (X_{Fe} < 0.02) occurs either as single elongated crystals or forms as a quartz-clinozoisite symplectite after grossular; clinozoisite shows an oblique extinction in thin sections, with an angle $X \wedge c$ less than 12°. In spite of abundant clinozoisite in the rock, only one sample contains this phase as inclusion in garnet. Both types of clinozoisite are not in direct contact with diamond-bearing garnet and kyanite suggesting clinozoisite and the quartz-clinozoisite symplectite formed in retrograde re-equilibration during rapid exhumation estimated to be less than 0.1 Ma. *P-T* estimates for garnet, clinopyroxene, clinozoisite, kyanite, biotite, potassium feldspar, quartz and for garnet, clinopyroxene, clinozoisite, biotite, potassium feldspar, quartz assemblages are 950°C at 2.0 GPa and 800°C at 0.7 GPa, respectively. Korsakov et al. (2002) suggests that clinozoisite either crystallized directly from melt or transformed from grossular according to a reaction, Cz + Qtz = Grs + melt, within the quartz stability field.

Epidote minerals in UHP felsic rocks. Compagnoni and Rolfo (1999) summarize some characteristics of UHP metapelite, gneiss and other unusual rocks from several UHP terranes. They pointed out that epidote minerals are generally stable in these lithologies at UHP conditions, including piemontite, which grows in Mn-rich compositions. Despite the felsic rocks described above for both Dabie-Sulu and Kokchetav, meta-sediments of the western Italian Alps contain clinozoisite-epidote ± sodic amphibole in addition to garnet and phengite as UHP stage minerals. Some oxidized manganiferous quartz-schists and quartzites have piemontite (X_{Mn} = 0.15–0.21 and X_{Fe} = 0.18–0.21) together with hematite, coesite, garnet, braunite, phengite, and rutile.

Pelagic metasediments and MORB-type metabasalts of the former Tethyan oceanic crust at Cignana, Zermatt-Saas Zone experienced UHP metamorphism at 615 ± 15°C and 2.8 ± 1.0 GPa (Reinecke 1991, 1998). The metamorphism resulted in the formation of coesite-glaucophane-eclogite in the basaltic layer and of garnet-dolomite-aragonite-lawsonite-coesite-

phengite-bearing calc-schist and garnet-phengite-coesite-schist with variable amounts of epidote, talc, dolomite, sodic pyroxene, and sodic amphibole in the overlying metasediments. In contrast to the well-preserved UHP metamorphic record of the coesite-glaucophane eclogite, the HP/UHP assemblages of the metasediments have been largely obliterated during exhumation. Relics from which the metamorphic evolution of the rocks can be retrieved are restricted to rigid low-diffusion minerals like garnet, tourmaline, and apatite (Reinecke 1998). Assemblages with dolomite, aragonite, lawsonite, phengite, apatite, tourmaline, talc and epidote/piemontite occurring in the calc schists and quartz-schists indicate that the metasedimentary rocks contained significant amounts of H_2O and CO_2 during the UHP stage. These assemblages may persist to more than 4 GPa; these hydrous phases may act as major carriers of fluids into mantle (e.g., Schmidt and Poli 1998).

Factors controlling the common occurrence of UHP epidote minerals. Paragenesis and compositions of epidote minerals in UHP rocks are controlled by P, T, f_{O_2}, and bulk rock composition. The common occurrence of UHP epidote in Dabie-Sulu is apparently related to the oxidized protoliths revealed from mineral assemblages. Such protoliths were obtained by hydrothermal alteration revealed from exciting findings of extraordinarily low $\delta^{18}O$ and δD values of UHP minerals, including epidote-zoisite (see Morrison 2004). Reported $\delta^{18}O$ values for eclogites worldwide range from +1.5 to +12.0‰ (see summary by Yui et al. 1995). However, analyses of $\delta^{18}O$ values for mineral separates from eclogite, gneiss, and quartzite from Dabie-Sulu yielded world-record negative $\delta^{18}O$ values of −2.1 to −11.1‰ for epidote, −4 to −11‰ for garnet, −2.2 to −11.2‰ for omphacite, −1.2 to −10.7‰ for phengite, 0.8 to −7.7‰ for quartz and −5.3 to −14.8 ‰ for rutile (Yui et al. 1995; Zheng et al. 1996; Baker et al. 1997; Rumble and Yui 1998; Zheng et al. 1999). Compiling the available data, Zheng et al. (2003) show that UHP eclogites and associated gneisses have $\delta^{18}O$ values ranging from −11‰ to +22%. These data cover the whole range of the major water reservoirs such as seawater (0 ‰), meteoric water (< −2 ‰, depending on latitude), magmatic water (+5 to +7‰), and marls (+25 to +35 ‰). Most of the unaltered samples preserve oxygen isotope equilibrium fractionations only on a mm-scale, yielding reasonable T estimates of 650–750°C responsible for UHP metamorphism. Some UHP rocks preserve pre-metamorphic differences in $\delta^{18}O$ at the outcrop scale, suggesting that closely spaced rocks have not achieved meter-scale isotopic re-equilibration during the entire metamorphic process (Rumble and Yui 1998). Together with low δD values (from −101 to −127 ‰), these characteristics are interpreted as follows. (1) The protoliths were once at or near the Earth's surface and were subjected to alteration in a geothermal area charged with meteoric water from a Neoproterozoic snowball Earth (Yui et al. 1995; Zheng et al. 1996; 1999, 2003; Rumble et al. 2002). (2) The persistence of pre-metamorphic differences in oxygen and hydrogen isotopic composition between different rocks and the preservation of high-T isotope fractionation between UHP minerals indicate a lack of flowing fluid to mediate isotope exchange between rocks during UHP and retrograde metamorphism (e.g., Getty and Selverstone 1994; Rumble and Yui 1998; Philippot and Rumble 2000). Thus, the environment for subduction of old supracrustal rocks constitutes an example of a fluid-deficient region of metamorphism (Yoder 1955). Other recent studies indicate that O-isotope disequilibrium between UHP minerals may have been caused by retrograde hydration (Yui et al. 1997; Zheng et al. 1999) and the difference in isotopic composition of eclogite protoliths in various areas was not only controlled by different degrees of water-rock interaction before metamorphism, but also by channelized flow of fluids during retrograde metamorphism due to rapid exhumation (Zheng et al. 1999, 2003).

Magmatic-hydrothermal alteration of the protoliths of Dabie-Sulu UHP rocks has been proposed (e.g., Rumble et al. 2002; Zheng et al. 2003). One example is rift-related magmatism along the northern margin of the Yangtze craton resulting in melting of glacier ice and triggering meteoric-hydrothermal circulation during Snowball Earth time. Channelized fluid flow caused a variable extent of water-rock interaction and different degrees of ^{18}O-depletion around

the Neoproterozoic magmatic system (e.g., see Bird and Spieler 2004 for fossil and active hydrothermal systems for epidote formation). In addition to lower $\delta^{18}O$ for some protoliths, such alterations caused oxidation of the protoliths including quartzite, granite, paragneiss, and associated basaltic rocks. These oxidized rocks are the sites for the formation of UHP epidote during Triassic subduction. Common occurrences of UHP epidote in both eclogites and epidote ± acmite in gneiss at the type locality of the $\delta^{18}O$ anomaly in the Qinglongshan area mentioned above and piemontite schist in the Mulanshan area of the southern Hongan block (e.g., Eide and Liou 2000) supports such a model. This process excludes the common occurrence of microdiamond in the Dabie-Sulu terrane in spite of UHP metamorphism within the diamond *P-T* stability field.

The effect of f_{O_2} on the stability of epidote is illustrated in Figure 21 for the epidote-bearing eclogites from Qinglongshan (Mattinson et al. in review). During eclogite-facies metamorphism, f_{O_2} is estimated using the reaction

$$12\ \text{Ep}\ (X_{Fe} = 0.33) = 8\ \text{Grs} + 4\ \text{Alm} + 3\ O_2 + 6\ H_2O$$

calculated using the THERMOCALC v2.5 program and data set of Holland and Powell (1990). Mineral activities were calculated from rim compositions of peak-stage garnet and epidote using the a-X program of Holland and Powell (1998); unit H_2O activity was assumed. The results indicate consistent, oxidized conditions for eclogite samples, approximately 2.5 log f_{O_2} units above the hematite-magnetite (HM) buffer over the calculated temperature range (Fig. 21a). This is consistent with the Mg-rich composition of early-retrograde amphibole. Conditions were too oxidizing for the persistence of graphite or the formation of diamond under peak conditions, although *P-T* estimates for several samples lie within the diamond stability field. The graphite-CO_2 buffer (at $X_{CO_2} = 1$) is approximately one log f_{O_2} unit below the HM buffer (Fig. 21a), and for X_{CO_2} appropriate for epidote stability (<0.04 at $P = 3$ GPa: see also Boundy et al. 2002), the graphite-CO_2 curve is approximately 1.5log f_{O_2} units lower.

The presence of Ti-hematite and the absence of magnetite and graphite in gneiss and quartzite samples are consistent with the f_{O_2} calculated for the eclogites. Rim compositions of

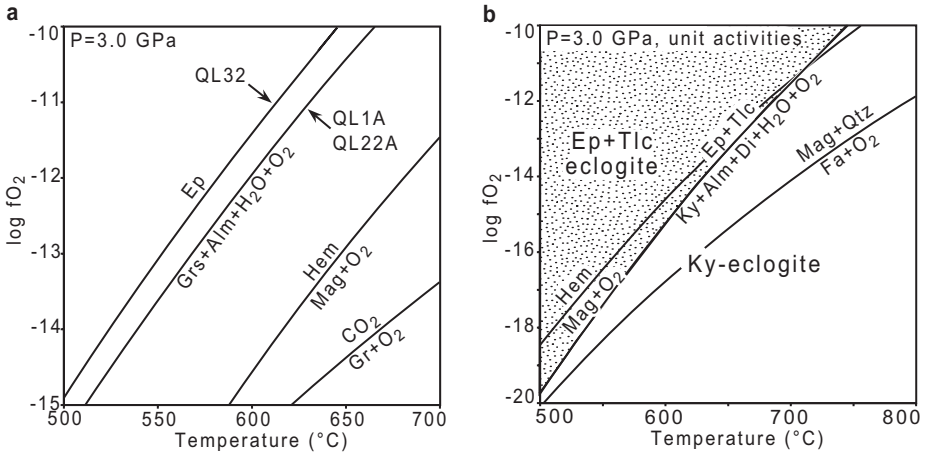

Figure 21. Log f_{O_2}-*T* diagrams calculated using THERMOCALC v. 2.5 program and data set of Holland and Powell (1990): (a) f_{O_2} estimates for Qinglongshan epidote-kyanite-talc eclogite samples (sample numbers indicated), calculated from mineral rim compositions. Diamond is stable below 515°C if f_{O_2} is sufficiently low; (b), f_{O_2}-*T* diagram calculated for unit activities. Ep + Tlc eclogites (stippled field) are the low temperature, high f_{O_2} equivalents of common kyanite eclogites.

garnet and epidote in gneiss indicate slightly more oxidized conditions (if calculated at 3 GPa) than eclogitic samples; compositions of Ti-hematite and garnet included within it indicate f_{O_2} conditions identical to that of eclogitic garnet-epidote pairs. The garnet-epidote reaction shifts by approximately 0.005log f_{O_2} unit/GPa relative to the HM buffer over the pressure range 0.1 to 2.0 GPa (Donohue and Essene 2000). The reaction

$$8\ \mathrm{Tlc} + 12\ \mathrm{Ep}\ (X_{\mathrm{Fe}} = 0.33) = 24\ \mathrm{Di} + 4\ \mathrm{Alm} + 8\ \mathrm{Ky} + 3\ O_2 + 14\ H_2O$$

(calculated for unit activities) shows that epidote-talc eclogites are low-temperature oxidized equivalents of the more common kyanite eclogites (Fig. 21b). Garnet-epidote estimates of f_{O_2} in eclogite-facies carbonate rocks (1.8–2.0 GPa/580–690°C) from the Norwegian UHP terrane indicate oxidizing conditions 0.3 to 1.0 log f_{O_2} unit above the HM buffer (Donohue and Essene 2000, Boundy et al. 2002). This suggests that calculated f_{O_2} for the Qinglongshan samples are not unreasonable.

Interaction with oxidized, meteoric water in a hydrothermal system such as that hypothesized by Rumble et al. (2000) may be responsible for oxidation and hydration, as well as $\delta^{18}O$ depletion, of the Qinglongshan epidote-talc eclogite protoliths. If this is correct, combined oxygen isotope analysis and f_{O_2} calculation should reveal that the $\delta^{18}O$ of relatively reduced eclogites is higher than that of oxidized, epidote-talc eclogites. Heterogeneity of hydrothermal alteration combined with lack of extensive fluid flow during UHP metamorphism can explain the presence of epidote-free eclogites surrounded by epidote-talc eclogites, as well as the preservation of anomalously low, pre-metamorphic isotopic values in this region.

Retrograde stages (stages III and IV)

Epidote minerals are common products of retrograde amphibolite to greenschist facies overprint during exhumation. Depending on the bulk composition of the host rock, retrograde epidote minerals in veins or in the matrix vary in composition. Some gneisses in Dabie are transformed from quartz-rich eclogite through retrograde hydration, metasomatism and crystallization of secondary minerals to hornblende-biotite-epidote gneiss (Zhang et al. 2003). The layered rock series consists of various intercalated eclogite, paragneiss, granitic gneiss, jadeite quartzite and marble with or without eclogite nodules (Cong et al. 1995). The eclogite contains abundant coesite relics in garnet and omphacite; all lithologies including epidote-bearing gneisses were subjected to *in situ* UHP metamorphism and multistage retrograde re-equilibration (Carswell et al. 2000).

Zhang et al. (2003) investigated a series of variably retrograded eclogites and gneissic rocks from a single outcrop of about 20 thin layers of mafic and felsic rocks with various compositions and extent of retrogression and its nearby localities. These eclogites are extensively retrograded; most omphacite grains are completely replaced by amphibole and plagioclase. Several layers of epidote-bearing gneissic rocks concordant with eclogite layers consist mainly of quartz and aggregates (or domains) of fine-grained amphibole, plagioclase, epidote, biotite, titanite, and ± calcite. Based on mineral constituents and shapes of domains, they are interpreted as pseudomorphs after garnet, omphacite, kyanite and rutile. Gneiss with coarse-grained quartz and pseudomorphs after garnet and omphacite exhibit strong deformation. Some plagioclase-epidote-amphibolite-biotite pseudomorphs after garnet contain skeletal to irregular garnet relics. Garnet domains with garnet relics are surrounded by amphibole and plagioclase or by amphibole, plagioclase, epidote, and biotite. Based on analyzed compositions and texture, such retrogressive reaction of garnet and omphacite may be written

$$\mathrm{Grt} + \mathrm{Omp} + H_2O = \mathrm{Pl} + \mathrm{Amph} \pm \mathrm{Cpx}$$

Another possible transformation involves the reaction of almandine and grossular components of garnet with H_2O to produce epidote ± amphibole, whereas the excess Fe and

Mg react with K of the fluid or phengitic mica to form biotite. Subsequent hydration reaction for the replacement of garnet by epidote and biotite can be written as

$$\text{Amph} + \text{Grt} = \text{Ep} + \text{Bt} \quad \text{or}$$

$$\text{Amph} + \text{Grt} = \text{Chl} + \text{Pl} + \text{Bt}$$

The replacement of kyanite by zoisite, muscovite/biotite, and sodic plagioclase can be written as

$$6\,\text{Ky} + 8\,\text{Omp} + \text{K}_2\text{O} + 2\,\text{SiO}_2 + 3\,\text{H}_2\text{O} = 2\,\text{Zo} + 2\,\text{Ms} + 4\,\text{Ab} + 4\,\text{MgO} \quad \text{or}$$

$$4\,\text{Ky} + 8\,\text{Grt} + 8\,\text{SiO}_2 + 2\,\text{K}_2\text{O} + \text{Na}_2\text{O} + 7\,\text{H}_2\text{O} = 6\,\text{Zo} + 4\,\text{Bt} + 2\,\text{Ab}.$$

Epidote biotite gneiss is characterized by pronounced foliation, and near equigranular texture. It is composed of biotite flakes (15 vol%) (+ minor muscovite), quartz, plagioclase, microcline, apatite, and coarse-grained epidote (up to 1 mm) pseudomorphic after coarse-grained garnet. Ghost habits of garnet and omphacite domains become obscure; the size of individual crystals including plagioclase, epidote and biotite in these domains are larger than those in the extensively retrograded eclogites. Only rare garnet domains could be recognized as trace garnet relics are embayed by aggregates of plagioclase + epidote + hornblende + biotite. Such aggregates in gneissic rocks represent products of retrograde reaction in a closed system with introduction of H_2O. However, for pseudomorphs with high biotite contents, additional potassium metasomatism must be evoked.

EPIDOTE MINERALS AS AN INDICATOR OF FLUID-ROCK INTERACTION AND PARTIAL MELTING

Zoisite and clinozoisite occur in segregations and pegmatitic veins in HP-UHP metamorphic rocks. They obviously point to high fluid activity at these conditions, and are a key to discuss high-*P* fluid-rock interaction and partial melting process of metamorphic rocks during exhumation stage. Zoisite and clinozoisite segregations are widely distributed in HP-UHP metamorphic rocks of the Tauern Window, and have been well documented (e.g., Selverstone et al. 1992; Brunsmann et al. 2000).

In the Eclogite Zone of the Tauern Window, abundant small (cm-10 cm scale) segregations with variable mineral assemblages, including zoisite (X_{Fe} = 0.03–0.06) + clinozoisite (X_{Fe} = 0.10–0.22) + rutile, are observed in banded and massive eclogites (Selverstone et al. 1992). These are localized fractures and are not linked to any through-going fractures. The formation conditions of the segregates are roughly estimated as 2 GPa and 600°C. Zoisite and clinozoisite occur as euhedral blasts up to 1 mm in length and smaller subhedral to euhedral grains radiating inwards from the wall of the segregation, respectively. Zoisite frequently shows sector-zoning and patchy extinction. Close similarities in mineralogy and mineral chemistry between the segregations and their host eclogites, and the absence of metasomatic halos surrounding the segregations imply that the zoisite and clinozoisite segregations crystallized from a metamorphic fluid phase that was in equilibrium with the host rocks. Selverstone et al. (1992) interpreted the segregations to be fractures produced by local solution and precipitation of material either during hydrofracturing associated with devolatilization in the host eclogites, or in response to ponding of non-wetting fluids in certain of the layers. Thus the segregations might be an evidence for at least instantaneous conditions of $P_{fluid} > 2$ GPa.

High-*P* zoisite- and clinozoisite-bearing segregations (mm-cm scale) are common in garnet- and albite-bearing amphibolites of the Lower Schieferhülle of the Tauern Window (Brunsmann et al. 2000), which equilibrium conditions are slightly lower (0.6–1.2 GPa/400–550°C) than the Eclogite Zone. Formation history of these segregations is more complicated

than in the Eclogite Zone. The zoisite segregations (primary assemblage: zoisite with X_{Fe} = 0.03–0.06 + quartz + calcite) formed during an early to pre-Hercynian high-*P* event (> 0.6 GPa/500–550°C) by hydrofracturing as a result of protolith dehydration. Most contacts between the zoisite segregations and host rock are sharp, but some are slightly diffuse over a few mm in width. The clinozoisite segregations (primary assemblage: clinozoisite with X_{Fe} = 0.10–0.19 + quartz + omphacite + titanite + chlorite + calcite) are commonly crosscutting the fabrics of the host amphibolite. They formed during the Eoalpine high-*P* event at 0.9–1.2 GPa/400–500°C.

Zoisite- and clinozoisite-bearing pegmatites in eclogites are well documented from the Münchberg Massif (Franz and Smelik 1995). The peak metamorphic conditions of the host eclogites are estimated at 2.5 GPa/600–700°C (e.g., O'Brien 1993). Zoisite occurs as large (up to 10 cm in length) euhedral crystals in a matrix of quartz and plagioclase with abundant graphic intergrowths. It is zoned with core (X_{Fe} = 0.06) and inner rim (X_{Fe} = 0.04)-outer rim (X_{Fe} = 0.03), which boundary is very sharp and mimics the outline of the entire crystal (Fig. 22). Most clinozoisite crystals (X_{Fe} = 0.10–0.13) occur as parallel intergrowths within the zoisite crystal with very sharp interface, and are commonly associated with albite and occasionally with calcic amphibole. Small (on the order of 100 μm) crystals of clinozoisite have grown at the rims of the zoisite crystal, especially where they are corroded. The graphic texture of the zoisite- and clinozoisite-bearing pegmatites, their large grain size, and their contact relationships with the country rocks all indicate igneous origin for the pegmatites, showing strong evidence for partial melting caused by isothermal decompression during exhumation (Fig. 22).

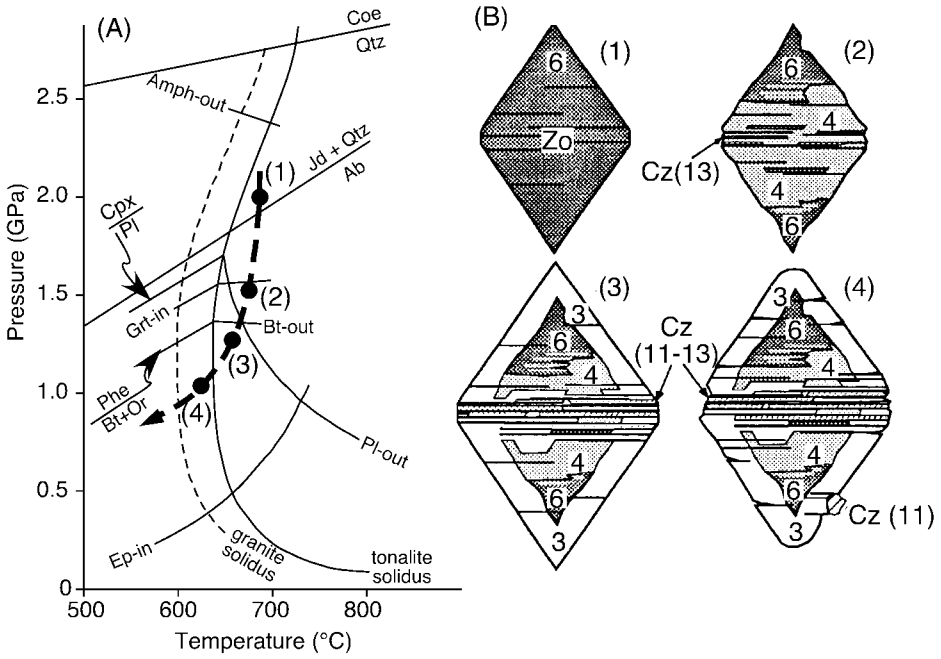

Figure 22. (A) *P-T* path of eclogites from the Münchberg Massif during exhumation leading to partial melting and pegmatite formation, and (B) progression of zoisite growth during four stages of pegmatite formation (modified from Fig. 4 of Franz and Smelik 1995). Numbers indicate $X_{Fe} \times 100$.

SOME PECULIAR CRYSTALCHEMICAL ASPECTS OF HP TO UHP EPIDOTE MINERALS

Compositional variations within the A(2)-site

Monoclinic epidote minerals have two distinct sites commonly occupied by Ca: the seven- to ninefold-coordinated A(1) and eight- to tenfold-coordinated A(2) sites. The A(2) site is slightly larger than the A(1) site, and its size increases with incorporation of Fe^{3+} and Mn^{3+} in octahedral M(1) and M(3)-sites. The A(2)-site can readily incorporate Sr (1.36 Å) and larger cations as indicated by the occurrence of niigataite, a Sr analog of clinozoisite in high *P*/*T* metamorphic rocks (Miyajima et al. 2003). In the Sanbagawa schists described above, considerable amounts of Sr and other divalent elements are detected in epidote minerals (Fig. 23, Table 3). The maximum Sr content of Al-Fe^{3+} solid solutions ($Fe^{3+} > Mn^{3+}$) is 0.24 pfu (5.0 wt% SrO), whereas the Ba content is usually below the detection limit of the microprobe analysis (0.08 wt% for 2σ level). In normal piemontite ($Fe^{3+} + Mn^{3+} \geq 1$ and $Mn^{3+} > Fe^{3+}$) Sr ranges from 0.00 to 0.36 pfu (0.0–7.3 wt% SrO). Even higher Sr contents are found in strontiopiemontite. Strontium, Ba, and Pb contents are 0.43–0.71 pfu (up to 13.1 wt% SrO),

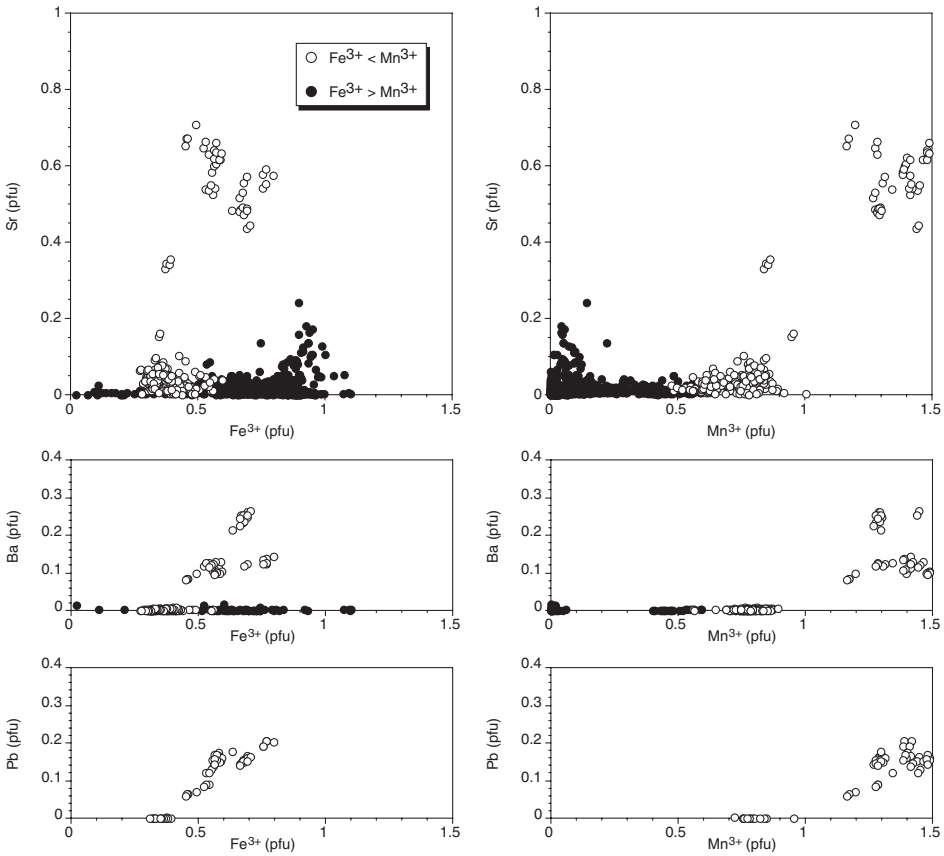

Figure 23. Relationship between (Fe^{3+}, Mn^{3+}) and (Sr, Ba, Pb) of epidote minerals from the Sanbagawa belt (Enami and Banno 2001; Enami unpublished data). Pb contents of epidote with $Fe^{3+} > Mn^{3+}$ are not analyzed.

0.08–0.26 pfu (up to 7.0 wt% BaO), and 0.06–0.20 pfu (up to 7.7 wt% PbO), respectively. The X_{Al} value of strontiopiemontite is 0.36 ± 0.05, and the X_{Fe} and X_{Mn} values are 0.15–0.27 and 0.36–0.48, respectively. This implies as ideal formula $(Sr,Ba,Pb)Ca(Mn^{3+},Fe^{3+})_2AlSi_3O_{12}(OH)$. The Ba and Pb substitutions in the strontiopiemontite are described by the hypothetical end-members for epidote minerals "Ba-piemontite" [$BaCa(Mn^{3+}, Fe^{3+}, Al)_2AlSi_3O_{12}(OH)$] and "Pb-piemontite [$PbCa(Mn^{3+}, Fe^{3+}, Al)_2AlSi_3O_{12}(OH)$]" (Fig. 24, Table 2; Enami and Banno 2001).

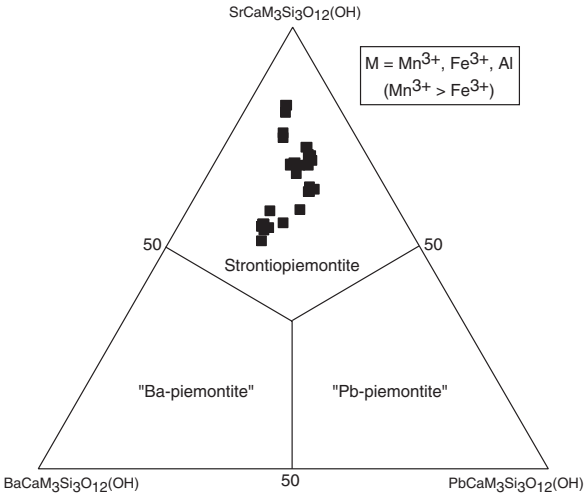

Figure 24. Compositional range of Sr, Ba, and Pb-bearing piemontite ($Mn^{3+} > Fe^{3+}$) in quartz schist from the Sanbagawa belt (modified from Fig. 7 of Enami and Banno 2001).

Sector-zoning of epidote minerals

Sector-zoned zoisite is described in a metagabbro at Fujiwara, central Shikoku, from the Sanbagawa belt (Enami 1977). The metagabbro occurs near the boundary between the garnet and albite-biotite zone and its metamorphic conditions are equivalent to lower-grade epidote-amphibolite facies. The typical mineral assemblage coexisting with zoisite is diopside, hornblende, chlorite, albite, and quartz. It is difficult to find this sector structure using polarizing microscopy in normal thin sections. However, in slightly thicker thin sections, the sector structure is easily observed from the differences of interference colors among the sectors (Fig. 25). Zoisite is composed of three square pyramids of {100}, {010} and {001} named after their growing surfaces. Each sector is composed of a core and Fe^{3+}-richer mantle. In the core of each sector, X_{Fe} decreases towards the outer margin. The X_{Fe} of sectors increases in the order of {001} < {010} < {100}.

Sector-zoning is also observed in epidote of the Sanbagawa mafic schists from the chlorite zone (Fig. 26; Yoshizawa 1984). The epidote is fine-grained (less than 100 μm in length), and composed of sector-zoned cores and non-sector-zoned rims. The sector structure is best seen using polarizing microscopic observation of polished thin sections. X_{Fe} decreases in the order {100}, {110}, {001} and $\{10\bar{1}\}$ sectors from the core, and non-sector-zoned rim areas.

It is likely that compositional sector-zoning of epidote minerals is easily overlooked in regular thin sections and it may be more common in epidote of low-grade zone in HP metamorphic rocks than currently realized (Banno and Yoshizawa 1993). Compositions of epidote especially in low-grade metamorphic rocks are typically quite variable both in single

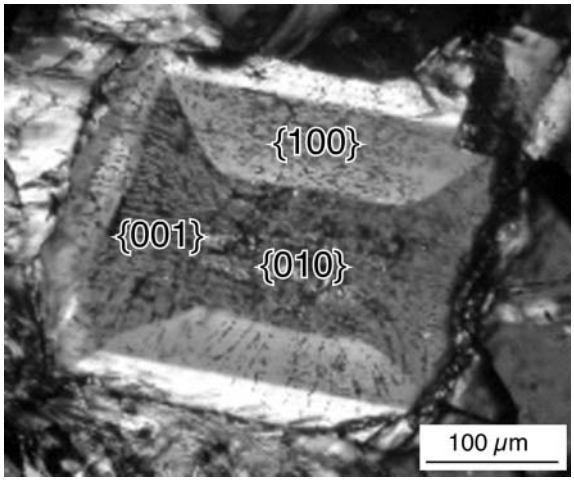

Figure 25. Photomicrograph (crossed polarized light) of a sector-zoned zoisite in (010) section from the Fujiwara metagabbro in the Sanbagawa belt reported by Enami (1977). The sector-zoned zoisite is composed of three types of rectangular pyramid. Symbol {*hkl*} indicates basal plane of the pyramid.

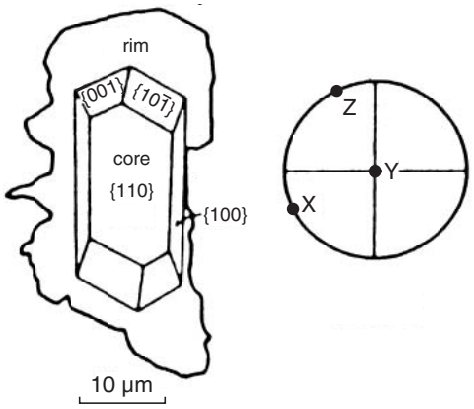

Figure 26. Sketch of sector-zoned epidote in (010) section from mafic schist in the Sanbagawa belt (modified from Fig. 3 of Yoshizawa 1984). The sector-zoned core is mantled by non-sector-zoned rim. Optical orientation of the section is shown in stereographic projection.

grains and within a single thin section (e.g., Fig. 11), and this may be in part due to sector-zoning. Thus, in Sanbagawa rocks sector-zoned epidote indicates disequilibrium growth, and care needs to be exercised in establishing equilibrium compositions.

LAWSONITE-EPIDOTE RELATIONS

The *P-T* region of the blueschist facies is subdivided into lawsonite and epidote blueschist facies and this subdivision is qualitatively correlated with increasing grade. Lawsonite-bearing blueschist forms at a temperature below 375°C and epidote bearing, lawsonite-free blueschist at a higher temperature of up to 500°C (Evans 1990).

Textural replacement of lawsonite by later epidote or lawsonite growth from epidote have been documented in many major blueschist terranes, for example, in the Swiss, Tauern Window, Austrian-Italian Alps by Selverstone and Spear (1985), in Alaska by Thurston (1985), and in

the Armorican Massif, France by Ballevre et al. (2003). Similarly, retrograde replacement of epidote by lawsonite in high-grade tectonic blocks is also common in the Franciscan Complex as described above. These relationships suggest two episodes of metamorphic re-equilibration where epidote and lawsonite are not in equilibrium. On the other hand, because of the slight compositional difference between these two phases, minor differences in f_{O_2} during blueschist facies metamorphism, and the small domain size of equilibrium in low-T metamorphic rocks, both lawsonite and epidote can be in equilibrium in blueschist (e.g., Brown 1977; see also discussion of this topic in Poli and Schmidt 2004).

Ca-Al-silicates in high P/T metamorphic terranes include lawsonite, pumpellyite, epidote minerals and prehnite. Their occurrence has been used as an index mineral to map progressive metamorphic zones for metabasite, e.g., Franciscan, Sanbagawa, New Zealand, and New Caledonia (e.g., Maruyama et al. 1996). For the Franciscan metabasites in Ward Creek as described above, there is a progressive sequence from lawsonite through pumpellyite to an epidote zone. Progressive order of pumpellyite through lawsonite to epidote also occurs in New Caledonia, pumpellyite to epidote zone in Sanbagawa, and prehnite through pumpellyite to epidote with local lawsonite in New Zealand.

In blueschist-facies metamorphism, lawsonite occurs in low-grade blueschist, whereas epidote is common in high-grade blueschist, epidote-amphibolite and eclogite (Evans 1990). The relationship between zoisite and lawsonite has been experimentally determined (e.g., Schmidt and Poli 1994; Okamoto and Maruyama 1999) and thermodynamically calculated. The occurrence of epidote vs. lawsonite in Franciscan blueschist-facies rocks was investigated by Brown and Ghent (1983) and Maruyama and Liou (1987). Lawsonite occurs in nearly all lithologies in Pacheco Pass (e.g., Ernst et al. 1970) which display a high P/T gradient (< 12°C/km) whereas epidote is ubiquitous in Shuksan blueschist (Washington) that has a relatively low P/T gradient (> 12°C/km). An intermediate P/T gradient of the South Fork Mountain Schist (~ 0.7 GPa /250–300°C) of the northern California Coast Range has produced a variety of assemblages including epidote + lawsonite + pumpellyite together with other blueschist-facies minerals. Metaclastics contain the dominant assemblage quartz, albite, chlorite, phengite, and lawsonite with sporadic occurrence of aragonite and epidote. Mafic schists at Black Butte of northern California have the assemblage quartz, albite, chlorite, pumpellyite, sodic amphibole, and titanite. Actinolite is uncommon and does not coexist with epidote or sodic amphibole. Lawsonite occurs in some mafic schists but is not associated with sodic amphibole. Mafic schists from the Ball Rock area of northern California have similar assemblages with the notable exception that (1) lawsonite is common and coexists with sodic amphibole, and (2) epidote is less common. This control of the bulk composition on the appearance of lawsonite, pumpellyite, and/or epidote in blueschist-facies assemblages is apparent from the Ca-Al-Fe^{3+} diagram (Fig. 27; Brown 1986; Maruyama and Liou 1987, 1988).

In addition to the effect of bulk rock composition, differences in f_{O_2} and X_{CO_2} also control the occurrence of lawsonite vs. epidote in different domains of a single outcrop. Chlorite and calcite at high X_{CO_2} replace both lawsonite and epidote. A simple reaction such as

$$\text{Lws} + \text{Fe-oxides} = \text{Ep} + \text{Qtz} + \text{Ky} + H_2O$$

was used to depict the lawsonite-epidote transition at low X_{CO_2}. This is shown schematically for a hypothetically metamorphosed pillow-lava overlain by pelagic sediment (Fig. 28; Liou 1993). The assemblage lawsonite, magnetite, and glaucophane (+ chlorite, albite, and quartz) occurs in pillow cores, epidote, crossite, and magnetite in pillow rims and hematite, epidote, acmite, and riebeckite (+ quartz) in overlying metapelagic sediments. The variation in f_{O_2} during blueschist-facies metamorphism may have been inherited from differences in the Fe^{3+}/Fe^{2+} ratio of the protoliths, which in turn may be controlled by differences in the degree of water/rock interaction and effective water/rock ratio. Variation in the mineral assemblage

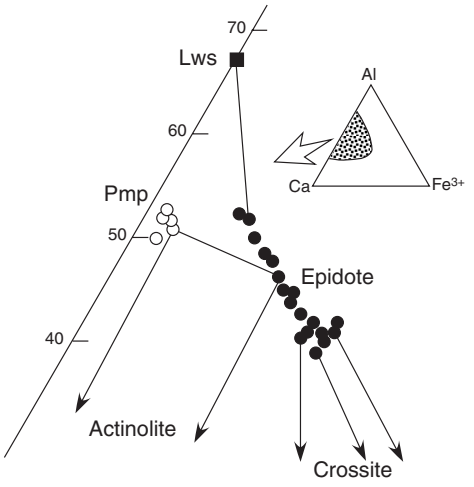

Figure 27. Phase relations of epidote (filled circles), lawsonite (filled square), and pumpellyite (open circles) in a Ca-Al-Fe^{3+} diagram projected from quartz, albite, chlorite, and H_2O, from the Shuksan Suite, Washington (modified from Fig. 7 of Brown 1986).

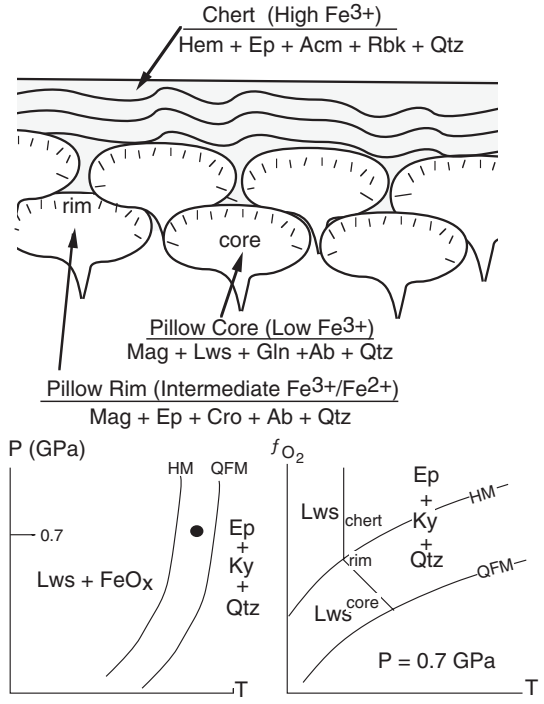

Figure 28. Schematic diagrams illustrating the effect of different f_{O_2} in local domains on the occurrence of lawsonite assemblages in a metamorphosed pillow core, epidote assemblages in the pillow rim and in overlying chert at constant P and T (modified from Fig. 7 of Liou 1993)

at constant P of about 0.7 GPa and 300°C in a single outcrop is due to difference in f_{O_2} (Fig. 28). Under highly oxidizing conditions such as in metapelagic sediments including hematite-bearing chert, the hematite, epidote, acmite assemblage appears in the lawsonite P-T stability field at $T < 300$°C.

PARAGENESIS OF EPIDOTE-CLINOZOISITE IN THE BLUESCHIST-GREENSCHIST TRANSITION

The P-T field of the blueschist facies is bounded by 4 to 5 other facies including the eclogite, epidote-amphibolite, greenschist, pumpellyite-actinolite facies and probably the prehnite-pumpellyite facies. Petrogenetic grids for these facies have been established (e.g., Oh and Liou 1990; Spear 1993). The blueschist facies occupies a large P-T space at $T < 500$°C and $P > 0.5$ GPa. All blueschist-facies boundary reactions contain both epidote and glaucophane on the blueschist-facies side. Thus, the blueschist-facies P-T field expands towards higher-T and lower-P in Fe^{3+}-rich rocks as epidote and glaucophane tend to preferentially incorporate Fe^{3+} compared to other silicates that define facies boundary reactions. Boundary reactions depend on what oxide phases develop; if magnetite or hematite is included, the P-T field of the blueschist facies expands (e.g., Banno and Sakai 1989).

Occurrences of two amphiboles (actinolite + sodic amphibole) together with epidote, chlorite, albite, titanite, and quartz in high P/T rocks are common. Depending on the textural relationship between the amphiboles, two stages of metamorphic re-equilibration have been documented with blueschist-facies conditions followed by those of the greenschist facies, such as in the Swiss Alps (e.g., Ernst 1973; Dal Piaz and Lombardo 1986), Sanbagawa (e.g., Ernst et al. 1970; Otsuki and Banno 1990), and Catalina Island (Sorensen 1986), or vice versa as in Anglesey, U.K. (Gibbons and Gyopari 1986). However, both blueschist and greenschist facies assemblages may be stable in a transitional P-T field, and coexisting sodic amphibole and actinolite define a miscibility gap in calcic amphibole (Liou and Maruyama 1987). Depending on bulk rock Fe^{3+}/Al ratio, blueschist, greenschist and transitional facies assemblages may be interlayered on a cm-scale and may form during a single metamorphic episode (Brown et al. 1982; Dungan et al. 1983; Oberhänsli 1986; Barrientos and Selverstone 1993). The textural relationship of the two amphiboles from the Ward Creek epidote-zone metabasites exemplifies their coexistence.

We use the blueschist-greenschist transition equilibria to illustrate the usage of epidote as a possible geobarometer described below. The boundary reaction

$$Cz + Gln + Qtz + H_2O = Act + Chl + Ab$$

was first proposed by Miyashiro and Banno (1958). The reaction is trivariant for natural metabasite; hence greenschist and blueschist assemblages could be interlayered as mentioned above. For a model basaltic system illustrated by the CaO-Al_2O_3-MgO diagram, the transition between blueschist and greenschist assemblages is defined by the univariant reaction

$$Cz + Gln + Qtz + H_2O = Tr + Chl + Ab \quad (1)$$

If Fe^{3+} is introduced into the system, the reaction

$$Ep + Mrb + Chl + Qtz = Tr + Ab + Hem + H_2O \quad (2)$$

The reaction (2) limits the low-P stability of sodic amphibole in metabasite. At P lower than that for this discontinuous reaction, metabasites do not contain magnesioriebeckite due to the stable coexistence of hematite and tremolite.

The blueschist-greenschist facies transition equilibria are bounded by the above two reactions in the model-Fe_2O_3 system (Fig. 29). Their P-T locations were estimated by Brown (1974,

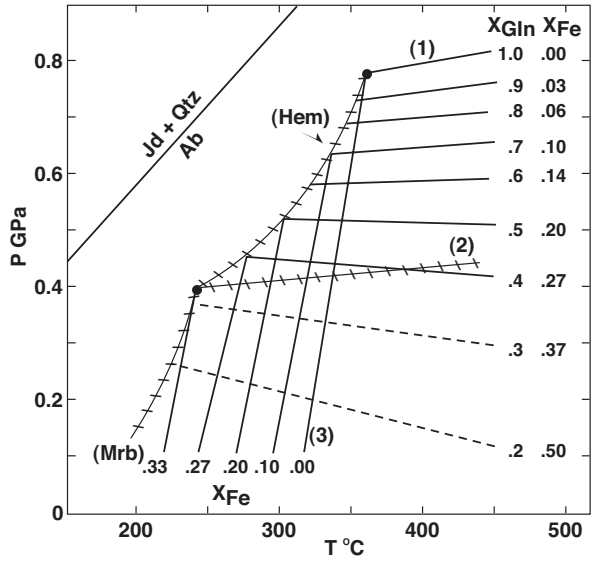

Figure 29. *P-T* diagram showing calculated compositions of coexisting epidote (X_{Fe}) and sodic amphibole (X_{Gln}) for the blueschist and greenschist transition assemblage of reaction (1) 6 Cz + 25 Gln + 7 Qtz + 14 H_2O = 6 Tr + 9 Chl + 50 Ab. Lines with hatch marks designated as (Hem), (Mrb) and (2) 4 Ep + 5 Mrb + Chl + 7 Qtz = 4 Tr + 10 Ab + 7 Hem + 7 H_2O are discontinuous reactions for the Fe_2O_3-saturated system. Lines designated as (3) are X_{Fe} isopleths of epidote for the pumpellyite-actinolite and greenschist transition assemblage (modified from Fig. 10 of Maruyama et al. 1986).

1977) based on natural paragenesis and were experimentally determined by Maruyama et al. (1986). Both reactions possess similar *P-T* slopes but reaction (1) occurs at much higher pressure than reaction (2). Therefore, a greenschist-blueschist transitional assemblage of sodic amphibole, actinolite, and epidote (+ albite, chlorite, and quartz) occurs in the *P-T* region between these two reactions. Because compositions and relative proportions of these phases for a given bulk composition change systematically along the continuous reaction (1) as a function of *P* and *T*, blue amphibole and epidote can be used to estimate the pressure.

POTENTIAL OF EPIDOTE MINERALS FOR THERMOBAROMETRY

The compositions of sodic amphibole and epidote are a function of pressure (Fig. 30, at 300°C). At f_{O_2} conditions above the HM buffer, sodic amphibole may vary along the join glaucophane – magnesioriebeckite, tremolite may have a very limited Fe^{2+} substitution, and the stable iron oxide is hematite. P_3 (Fig. 30) refers to the equilibrium pressure at 300°C for the reaction (1) in the model system. With gradual introduction of Fe_2O_3 into the model system, this reaction is displaced continuously toward lower pressure, and both epidote and sodic amphibole become more Fe^{3+}-rich. In the Fe^{3+}-saturated system, the discontinuous reaction (2) occurs at about 0.4 GPa. As long as f_{O_2} is maintained above that defined by HM, the discontinuous reaction remains at fixed pressure isothermally and has fixed mineral compositions for a given bulk composition, and in a P-X_{Fe} diagram the discontinuous reaction appears as a horizontal line (Fig. 30). If compositional variations of sodic amphibole of the reaction assemblage can be calibrated with pressure, the composition of clinozoisite-epidote could be used as a geobarometer (see below).

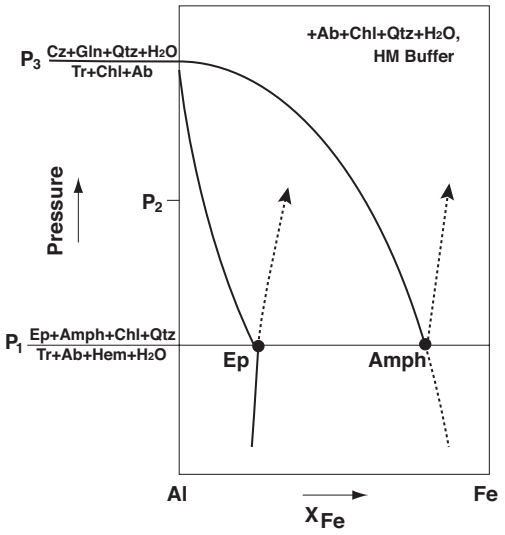

Figure 30. P-X_{Fe} plot at 300°C showing changes in compositions of sodic amphibole and epidote for buffered assemblages in the blueschist-greenschist transition: (1) the solid lines are for Ep + Tr + sodic Amph, and (2) the dashed lines for Ep + Hem + sodic Amph. P_1 and P_3 are, respectively, the equilibrium pressure for the discontinuous and continuous reactions for the facies transition (modified from Fig. 3.11 of Liou et al. 1987).

Phase assemblages with schematic tie-lines and compositions of sodic amphibole at P_1, P_2, and P_3 at 300°C are illustrated in ternary diagrams projected from chlorite (Maruyama et al. 1986; Fig. 31). Complete solid solution is assumed for the glaucophane – magnesioriebeckite and clinozoisite-epidote ($X_{Fe} = 0.33$) joins. These three diagrams illustrate the paragenetic and compositional variations of the blueschist-greenschist reaction assemblage as a function of not only pressure described above but also of bulk composition. For example, basaltic rocks have compositions between those of epidote and tremolite whereas ironstones may be very oxidized, containing abundant Fe_2O_3. At $P = P_3$ where the reaction (1) in the model system occurs (Fig. 31), basaltic rocks may contain the typical blueschist assemblage epidote and glaucophane (+ albite, chlorite, and quartz), whereas ironstones contain epidote, magnesioriebeckite, and hematite. At intermediate pressure (e.g., $P = P_2$), metabasites, depending on their bulk composition, may contain (l) the blueschist assemblage, (2) the greenschist assemblage, or (3) the reaction assemblage epidote, actinolite, and sodic amphibole where the composition of all three phases is fixed. If pressure decreases continuously, the Fe^{3+}/Al ratio of epidote and sodic amphibole varies systematically. When pressure is lowered to P_1, a discontinuous reaction occurs and compositions of the participating phases are fixed. At pressures lower than P_1, basaltic rocks with high Fe^{3+}/Al ratios contain the greenschist assemblage epidote, tremolite, and hematite whereas ironstones may have epidote, tremolite, and hematite or tremolite, magnesioriebeckite, and hematite depending on their bulk composition. Compositions of sodic amphibole from the basaltic 3-phase reaction assemblage epidote, actinolite, and sodic amphibole may differ significantly from those of ironstones. The composition of the former is shown as a solid line in Figure 30 for the basaltic sodic amphiboles and the latter compositions (ironstone amphiboles) as a dashed line.

The Fe^{3+}-Al partitioning between epidote and sodic amphibole for the reaction assemblage is complex (Maruyama et al. 1986). The effect of Fe^{3+}-Al substitutions of glaucophane and epidote solid solutions on the Al-end member reaction (1) can be expressed as

$$\ln K_{P_2} - \ln K_{P_1} = -\Delta V^{\circ} (P_2 - P_1)/\mathrm{R}T$$

where K_{P_2} and K_{P_1} stand for the equilibrium constants for the reaction at P_1 and P_2 respectively, ΔV° denotes the standard volume change for the reaction, and R and T represent gas constant

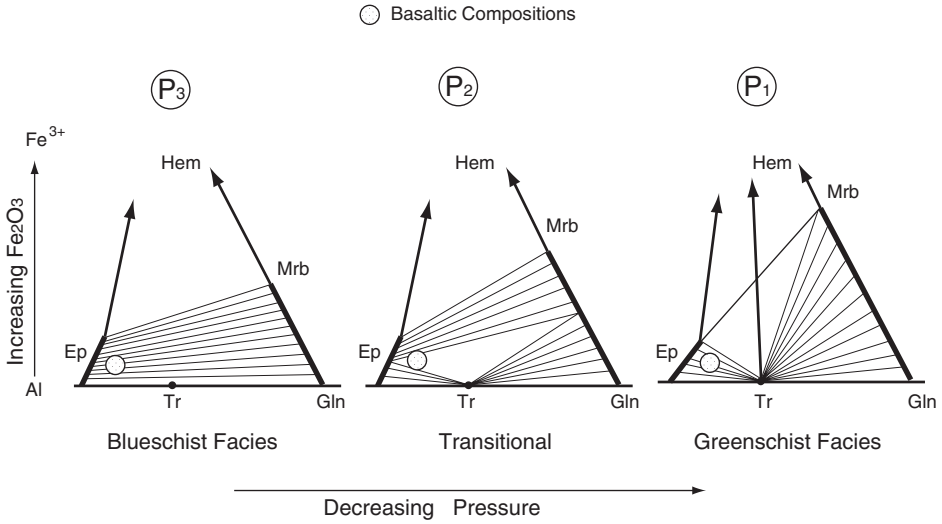

Figure 31. Schematic phase relations between hematite-epidote-amphibole in three isobaric sections at T = 300°C for the greenschist-blueschist transition (modified from Fig. 3.12 of Liou et al. 1987). For discussion as a geobarometer see text.

and T (in Kelvin) respectively. $\Delta V°$ is not constant in the dehydration reaction (1). As a first approximation, ΔV_{H2O} is assumed to be constant within a limited range of pressure (0.3–0.4 GPa) at a given temperature. This assumption results in error up to about 0.05 GPa in pressure estimates at 300–400°C, but may lie within the uncertainties of the experimental studies.

The intercrystalline partitioning of Fe^{3+}-Al cations between epidote and glaucophane of the buffered assemblage has to be maintained under equilibrium conditions. Hence, an additional constraint can be introduced by considering the exchange reaction such as

Gln + Ep = Mrb + Cz.

The isopleths of this sliding equilibrium were estimated assuming ideal substitution of Fe^{3+}-and Al cations in M(2)-sites for glaucophane solid solution and in both M(1) and M(3)-sites for epidote solid solution (for details, see Maruyama et al. 1986). Justification for such an assumption for epidote has been described by Nakajima et al. (1977). The isopleths illustrated in Figure 29 are drawn for constant composition for both epidote and sodic amphiboles in the buffered assemblage glaucophane, epidote, and actinolite (+ albite, chlorite, and quartz). The results indicate a rapid increase in Fe-content with decreasing pressure, especially at lower pressures. These isopleths of constant X_{Gln} and X_{Fe} do not give estimates of pressure consistent with those obtained from natural paragenesis. This apparent inconsistency may be due to the adopted ideal-composition relations as well as to other assumptions in the calculation. The isopleths have very gentle negative slopes at low pressures. Such a relation is very similar to those of the jadeite-albite-quartz sliding equilibrium. The gentle slope for these isopleths confirms their suitability as a geobarometer for the blueschist-greenschist facies transition. Both sodic amphibole and epidote in the buffered assemblage systematically increase in Al content with increasing pressure.

Also shown in Figure 29 are the isopleths related to a discontinuous reaction for a buffered assemblage epidote, actinolite, and pumpellyite (+ albite, chlorite, and quartz) from Nakajima et al. (1977). In contrast to the blueschist-greenschist transition, the isopleths for the

pumpellyite-actinolite and greenschist facies transition are very sensitive to temperature change, hence are good for geothermometer. Combination of these two sets of isopleths shown in Figure 29 provided better constraints for *P*-*T* relations in high *P*/*T* metamorphic facies series.

Pressure estimates from this geobarometer (Fig. 32; Maruyama et al. 1986) for epidote with X_{Fe} values of 0.13 to 0.19 in Franciscan metabasites yield ~0.7 GPa, whereas those with X_{Fe} = 0.31 to 0.38 in Mikabu of the Sanbagawa belt and New Zealand give pressure ~ 0.4 GPa. Glaucophane and clinozoisite were stable at higher pressures in Franciscan metabasites than were higher Fe^{3+} sodic amphibole and epidote in the Sanbagawa and New Zealand metabasites.

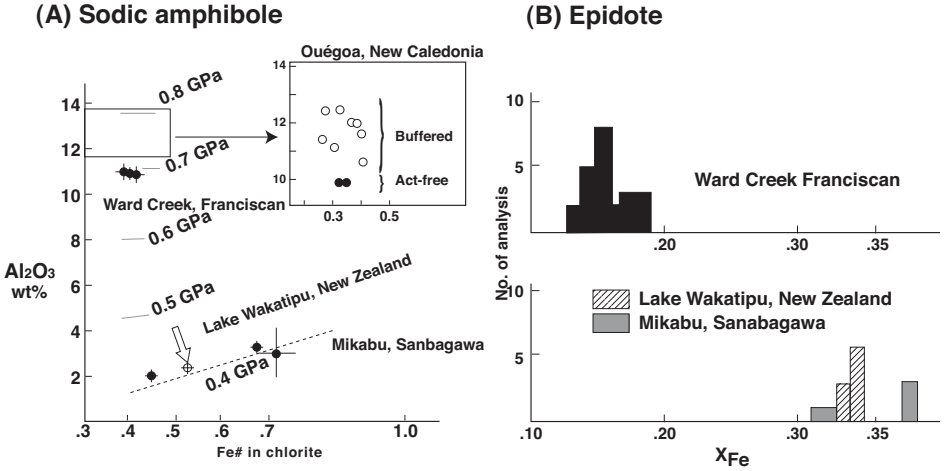

Figure 32. Mineral compositions of (A) sodic amphibole, chlorite and (B) epidote from the Sanbagawa, Franciscan, New Zealand and New Caledonia. Al_2O_3 wt% of sodic amphibole of the buffered assemblage sodic Amph + Act + Ep + Ab + Chl + Qtz is plotted against Fe# (= Fe/Fe + Mg) of chlorite. Pressure was estimated from pyroxene geobarometry. The composition of epidote from three of the blueschist terranes depends on pressure (modified from Fig. 3.17 of Liou et al. 1987).

EPIDOTE MINERALS AS CARRIERS OF TRACE ELEMENTS DURING SUBDUCTION

Epidote minerals contain several petrogenetically important trace elements as major elements (Frei et al. 2004) and are therefore important for the trace element budget of HP-UHP rocks. Allanite (see Gieré and Sorensen 2004) has also been reported in some UHP schists and orthogneisses hosting coesite-bearing eclogites from the Dabie-Sulu terrane of China (Carswell et al. 2000). The rare epidote mineral, dissakisite-(Ce), a Mg-analogue of allanite-(Ce) with up to 7.8 wt% MgO, was reported from a garnet-corundum rock (Enami and Zang 1988; Zhang et al. 2004) and garnet lherzolite (Yang and Enami 2003) of the Donghai area, Sulu terrane. It is the only REE-enriched phase in the examined samples, thus it is probably an important reservoir and carrier of REE in subducted and exhumed ultramafic rocks. The dissakisite-(Ce) in garnet lherzolite contains up to 5.4 wt% Cr_2O_3, and suggests the existence of a possible end-member "$CeCa(Mg,Fe)CrAlSi_3O_{12}(OH)$", in which both the highly incompatible REE as well as the highly compatible element Cr are incorporated.

As clearly indicated by occurrence of niigataite in a HP Omi-Renge metamorphic belt, Japan (Miyajima et al. 2003), epidote minerals in HP-UHP metamorphic rocks have the

potential to incorporate Sr as major component. For example, Sr-bearing epidote minerals are common constituents of eclogites and associated orthogneisses throughout the Sulu UHP terrane (Table 3: Nagasaki and Enami 1998). Prograde zoisite, epidote, and allanite have up to 3.2, 2.7 and 4.1 wt% SrO, respectively. They commonly show chemical zoning in which SrO content decreases from core to margin (Fig. 33). Retrograde epidote is poor in SrO (< 0.1 wt%). Apatite is always more depleted in SrO (0.10-0.59 wt% on average) than coexisting zoisite and epidote, and Sr-Ca partition coefficients for zoisite/epidote and apatite [(Sr/Ca)zo/ep-ap] range from 5 to 20. An evaluation of the SrO content in zoisite and epidote and their modal abundance indicates that > 70% of the whole-rock SrO is contained in epidote minerals. The characteristic Sr zonal structure of epidote minerals and high concentration of Sr into epidote minerals strongly suggest that zoisite and epidote are the main Sr reservoirs at HP-UHP conditions where calcic plagioclase is unstable and epidote minerals are main Ca-Al-silicates. Ca-poor, possibly Sr-rich zoisite and epidote have been commonly reported from the Dabie-Sulu terrane (e.g., Zhang and Liou 1994; Okay 1995). Thus, occurrences of Sr-bearing zoisite and epidote in UHP provinces may be widespread, and the presence or absence of these phases may strongly control the geochemical cycle of Sr in deep crustal and mantle environments (Hickmott et al. 1992).

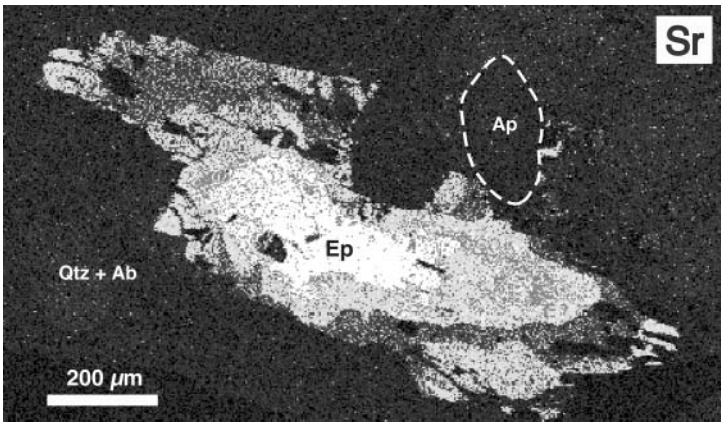

Figure 33. SrKα X-ray mapping image of epidote and coexisting minerals in an orthogneiss from the Sulu UHP terrane (after Fig. 3 of Enami 1999). Brighter shades indicate higher element concentration. SrO content ranges from 1.5-2 wt% in the core to less than 0.5 wt% in the margin.

CONCLUSIONS

Zoisite and epidote exhibit wide range of *P-T* stability and occurrences. Coexisting epidote and sodic amphibole, which is higher *T* equivalent of lawsonite + glaucophane, characterize mineral paragenesis of high-grade blueschist facies. Similarly, kyanite + zoisite + jadeite + SiO_2 assemblage is a common HP/UHP product of crustal plagioclase + H_2O in deeply subducted oceanic and continental materials. The maximum pressure limit of natural zoisite and epidote is not known; however, synthetic zoisite is stable to almost 7 GPa and natural epidote minerals coexist with coesite and/or microdiamond in UHP metamorphism. Thus epidote minerals are common Ca-Al-silicate in a variety of HP-UHP rocks recrystallized at the blueschist, epidote-amphibolite and eclogite facies. Only epidote minerals with inclusions of coesite or coesite pseudomorphs should be considered to be stable at UHP conditions. Previous descriptions list zoisite or clinozoisite in the peak UHP assemblage based

on petrographic observation and experimental studies; many reported analyses of epidote minerals do not include trace and REE element concentrations.

Epidote minerals in HP-UHP rocks have wide compositional ranges controlled by element substitutions in octahedral M(3)-site. Element proportion in the M(3)-site strongly depends upon Fe^{3+}/Al value of host rocks, which roughly correlates with the extent of oxidation during metamorphism. Epidote in low-f_{O_2}-rocks, such as graphite-bearing pelitic schists and pyrrhotite-bearing mafic schists, has $X_{Fe} < 0.2$, whereas most epidotes coexisting with hematite have $X_{Fe} > 0.3$. Piemontite is restricted to siliceous schist equilibrated under unusually high-f_{O_2} conditions that are inferred from the common occurrence of braunite and other highly oxidized phases. X_{Fe} of epidote minerals generally decreases with increasing metamorphic grade. In high-*P* pumpellyite-actinolite facies and low-grade blueschist facies, the decreasing X_{Fe} is probably advanced by continuous decomposition of pumpellyite and lawsonite, respectively. The principal factor responsible for decreasing X_{Fe} under high-grade greenschist facies and higher metamorphic grade conditions is not well known. Goto et al. (2002), however, emphasizes that calcite occurs in most Sanbagawa pelitic schists, and decarbonation reactions are the main factor responsible for increasing clinozoisite component in epidote with increasing metamorphic grade. The two-phase loop between zoisite and clinozoisite has funnel-like form, shifts towards Fe^{3+}-rich composition with increasing metamorphic temperature and pressure; zoisite represents the higher *T* and *P* phase in relation to epidote. Thus the frequency of appearance of zoisite increases with increasing metamorphic grade and zoisite commonly occurs in UHP metamorphic rocks.

Element substitutions into A(2)-site also control chemical composition of epidote minerals. Allanite is stable in HP-UHP metamorphic rocks and fulfills the role of an important REE reservoir for subducting oceanic and continental materials. Similarly, Sr-bearing epidote minerals are also common in HP-UHP metamorphic rocks, and are the main Sr reservoir. Therefore, epidote minerals may play the most important role in the cycling of some important trace elements in deep crustal and upper mantle environments. Moreover, as epidote minerals are stable to mantle depths, progressive changes of epidote-bearing assemblages at various depths in subducting oceanic and continental materials may affect the extent of mantle metasomatism, magma genesis and fluid transport above the subduction zone. Systematic microanalyses of REE and other trace element abundances of epidote minerals in HP and UHP rocks are essential to substantiate this conclusion.

Only the compositions of epidote from low-variance assemblages vary systematically with intensive variables and are controlled by continuous reactions, hence can be used as *P* or *T* indicators. Examples of such application have been suggested for blueschist and subgreenschist facies metabasite assemblages. Similar approaches should be extended to UHP conditions using both thermochemical calculations of pseudosections of the basaltic system and experimentally delineated phase equilibria as very limited geobarometers are available for UHP rocks.

ACKNOWLEDGMENTS

During the preparation of this review, many colleagues have contributed their ideas, data, figures and photos. We thank Ruyuan Zhang for photomicrographs of epidote with inclusions of coesite pseudomorphs, Diane Moore and Chang-Whan Oh for Franciscan epidote compositions and diagrams, and Liz Eide and Yupeng Yao for paragenetic diagrams for the Dabie-Sulu UHP belt. We also thank G. Franz, A. Liebscher, J. Selverstone, and R. Grapes for their constructive and critical reviews of this manuscript, and Shio Watanabe for drafting several diagrams. Preparation of this manuscript is supported in part by JSPS-14540448 and NSF EAR 0003355.

REFERENCES

Aoya M (2001) *P-T*-D path of eclogite from the Sambagawa belt deduced from combination of petrological and microstructural analyses. J Petrol 42:1225-1248

Baker J, Matthews A, Mattey D, Rowley D, Xue F (1997) Fluid-rock interactions during ultra-high pressure metamorphism, Dabie Shan, China. Geochim Cosmochim Acta 61:1685-1696

Ballevre M, Pitra P, Bohn M (2003) Lawsonite growth in the epidote blueschists from the Ile de Groix (Armorican Massif, France): a potential geobarometer. J Metamorphic Geol 21:723-736

Banno S, Sakai C (1989) Geology and metamorphic evolution of the Sanbagawa metamorphic belt, Japan. *In*: The Evolution of Metamorphic Belts. JS Daly, RA Cliff, BWD Yardley (eds) Blackwell Scientific Publications, Oxford, p 519-532

Banno S, Shibakusa H, Enami M, Wang Q, Ernst WG (2000) Chemical fine structure of Franciscan jadeitic pyroxene from Ward Creek, Cazadero area, California. Am Mineral 85:1795-1798

Banno S, Yokoyama K, Enami M, Iwata O, Nakamura K, Kasashima S (1976a) Petrology of the peridotite-metagabbro complex in the vicinity of Mt. Higashi-akaishi, Central Shikoku. Part I. Megascopic textures of the Iratsu and Tonaru epidote amphibolite masses. Sci Rept Kanazawa Univ 21:139-159

Banno S, Yokoyama K, Iwata O, Terashima S (1976b) Genesis of epidote amphibolite masses in the Sanbagawa metamorphic belt of central Shikoku. J Geol Soc Japan 82:199-210 (in Japanese with English abstract)

Banno S, Yoshizawa H (1993) Sector-zoning of epidote in the Sanbagawa schists and the question of an epidote miscibility gap. Mineral Mag 57:739-743

Barrientos X, Selverstone J (1993) Infiltration vs. thermal overprinting of epidote blueschists, Ile de Groix, France. Geology 21:69-72

Bird D, Spieler AR (2004) Epidote in geothermal systems. Rev Mineral Geochem 56:235-300

Black PM (1977) Regional high-pressure metamorphism in New Caledonia: phase equilibria in the Ouégoa district. Tectonophysics 43:89-107

Black PM, Brothers RN, Yokoyama K (1988) Mineral paragenesis in eclogite-facies meta-acidites in northern New Caledonia. *In*: Eclogites and Eclogite-facies Rocks. DC Smith, (ed) Elsevier, Amsterdam, p 271-289

Boundy TM, Austrheim H, Donohue CL, Essene EJ, Mezger K (2002) Discovery of eclogite facies carbonate rocks from the Lindås Nappe, Caledonides, Western Norway. J Metamorphic Geol 20:649-667

Brothers RN (1974) High-pressure schists in northern New Caledonia. Contrib Mineral Petrol 46:109-127

Brown EH (1974) Comparison of the mineralogy and phase relations of blueschists from the North Cascades, Washington and greenschists from Otago, New Zeland. Bull Geol Soc Amer 85:333-344

Brown EH (1977) Phase equilibria among pumpellyite, lawsonite, epidote and associated minerals in low grade metamorphic rocks. Contrib Mineral Petrol 64:123-136

Brown EH (1986) Geology of the Shukusan Suite, north Cascades, Washington, U.S.A. *In*: Blueschists and Eclogites. BE Evans, EH Brown, (eds) Geol Soc Am Memoir 164, p 143-154

Brown EH, Ghent ED (1983) Mineralogy and phase relations in the blueschist facies of the Black Butte and Ball Rock areas, northern California Coast Ranges. Am Mineral 68:365-372

Brown EH, Wilson DL, Armstrong RL, Harakal JE (1982) Petrologic, structural, and age-relations of serpentinite, amphibolite, and blueschist in the Shukusan Suite of the Iron Mountains-Gee Point area, north Cascades. Geol Soc Am Bull 92:1087-1098

Bruno M, Compagnoni R, Rubbo M (2001) The ultra-high pressure coronitic and pseudomorphous reactions in a metagranodiorite from the Brossasco-Isasca Unit, Dora-Maira Massif, Western Italian Alps: A petrographic study and equilibrium thermodynamic modeling. J Metamorphic Geol 19:33-43

Brunsmann A, Franz G, Erzinger J, Landwehr D (2000) Zoisite- and clinozoisite-segregations in metabasites (Tauern Window, Austria) as evidence for high-pressure fluid-rock interaction. J Metamorphic Geol 18: 1-21

Carswell DA, Wilson RN, Zhai M (2000) Metamorphic evolution, mineral chemistry and thermobarometry of schists and orthogneisses hosting ultra-high pressure eclogites in the Dabieshan of central China. Lithos 52:121-155

Castelli D, Rolfo F, Compagnoni R, Su X (1998) Metamorphic veins with kyanite, zoisite and quartz in the Zhu-Jia-Chong eclogite, Dabie Shan, China. Isl Arc 7:159-173

Clarke GL, Aitchison JC, Cluzel D (1997) Eclogites and blueschists of the Pam Peninsula, NE New Caledonia: a reappraisal. J Petrol 38:843-876

Coleman RG, Lanphere MA (1971) Distribution and age of high-grade blueschists, associated eclogites and amphibolites from Oregon and California. Geol Soc Am Bull 82:2397-2412

Coleman RG, Lee DE (1962) Metamorphic aragonite in the glaucophane schists of Cazedero, California. Am J Sci 260:577-595

Coleman RG, Lee DE (1963) Glaucophane-bearing metamorphic rock types of the Cazadero area, California. J Petrol 4:260-301

Compagnoni R, Rolfo F (1999) Characteristics of UHP pelites, gneisses, and other unusual rocks. Inter Geol Rev 41:552-570

Cong B, Zhai M, Carswell DA, Wilson RN, Wang Q, Zhao Z, Windley BF (1995) Petrogenesis of ultrahigh-pressure rocks and their country rocks at Shuanghe in Dabieshan, central China. Eur J Mineral 7:119-138

Dal Piaz GV, Lombardo B (1986) Early Alpine eclogite metamorphism in the Pennidic Monte Rosa-Gran Paradiso basement nappes of the northwestern Alps. *In*: Blueschists and Eclogites. BE Evans, EH Brown, (eds) Geol Soc Am Memoir 164, p 249-265

Deer WA, Howie RA, Zussman J (1986) Disilicates and Ring Silicates. Longman, London, 1B, p 629

Donohue CL, Essene EJ (2000) An oxygen barometer with the assemblage garnet-epidote. Earth Planet Sci Lett 181:459-472

Droop GTR (1985) Alpine metamorphism in the south-east Tauern window, Austria; 1. *P-T* variations in space and time. J Metamorphic Geol 3:371-402

Droop GTR, Lombardo B, Pognante U (1990) Formation and distribution of eclogite facies rocks in the Alps. *In*: Eclogite Facies Rocks. DA Carswell (ed) Blackie, Glasgow, p 225-259

Dungan MA, Vance JA, Blanchard DP (1983) Geochemistry of the Shuksan greenschists and blueschists, North Cascades, Washington; variably fractionated and altered metabasalts of oceanic affinity. Contrib Mineral Petrol 82:131-146

Eide EA, Liou JG (2000) High-pressure blueschists and eclogites in Hong'an: A framework for addressing the evolution of high- and ultrahigh-pressure rocks in central China. Lithos 52:1-22

Enami M (1977) Sector zoning of zoisite from a metagabbro at Fujiwara, Sanbagawa metamorphic terrain in central Shikoku. J Geol Soc Japan 83:693-697

Enami M (1978) Petrological study of epidote amphibolites and basic schists in the Besshi area, Sambagawa metamorphic terrain in central Shikoku. Master's Thesis, Kanazawa University, Kanazawa, p 152

Enami M (1980) Notes on petrography and rock-forming mineralogy (8) Margarite-bearing metagabbro from the Iratsu mass in the Sanbagawa belt, central Shikoku. J Japan Assoc Mineral Petrol Econ Geol 75: 245-253

Enami M (1983) Petrology of pelitic schists in the oligoclase-biotite zone of the Sanbagawa metamorphic terrain, Japan: phase equilibria in the highest grade zone of a high-pressure intermediate type of metamorphic belt. J Metamorphic Geol 1:141-161

Enami M (1986) Ardennite in a quartz schist from the Asemi-gawa area in the Sanbagawa metamorphic terrain, central Shikoku, Japan. Mineral J 13:151-160

Enami M (1999) CaAl-silicates: an important Sr container in subducted slab. J Geogr 108:177-187 (in Japanese with English abstract)

Enami M, Banno S (1980) Zoisite-clinozoisite relations in low- to medium-grade high-pressure metamorphic rocks and their implications. Mineral Mag 43:1005-1013

Enami M, Banno Y (2001) Partitioning of Sr between coexisting minerals of the hollandite- and piemontite-groups in a quartzose schist from the Sanbagawa metamorphic belt, Japan. Am Mineral 86:204-215

Enami M, Mizukami T, Yokoyama K (2004) Metamorphic evolution of garnet-bearing ultramafic rocks from the Gongen area, Sanbagawa belt, Japan. J Metamorphic Geol 22:1-15

Enami M, Wallis SR, Banno Y (1994) Paragenesis of sodic pyroxene-bearing quartz schists: implications for the P-*T* history of the Sanbagawa belt. Contrib Mineral Petrol 116:182-198

Enami M, Zang Q (1988) Magnesian staurolite in garnet-corundum rocks and eclogite from the Donghai district, Jiangsu province, east China. Am Mineral 73:48-56

Enami M, Zang Q, Yin Y (1993) High-pressure eclogites in northern Jiangsu-southern Shandong province, eastern China. J Metamorphic Geol 11:589-603

Ernst WG (1965) Mineral paragenesis in Franciscan metamorphic rocks, Panoche Pass, California. Geol Soc Am Bull 76:879-914

Ernst WG (1973) Interpretative synthesis of metamorphism in the Alps. Geol Soc Am Bull 84:2053-2078

Ernst WG, Seki Y, Onuki H, Gilbert MC (1970) Comparative study of low-grade metamorphism in the California coast ranges and the outer metamorphic belt of Japan, Geol Soc Amer Mem 124, p 276

Evans BW (1990) Phase relations of epidote-blueschists. Lithos 25:3-23

Franz G, Selverstone J (1992) An empirical phase diagram for the clinozoisite-zoisite transformation in the system $Ca_2Al_3Si_3O_{12}(OH)$-$Ca_2Al_2Fe^{3+}Si_3O_{12}(OH)$. Am Mineral 77:631-642

Franz G, Smelik EA (1995) Zoisite-clinozoisite bearing pegmatites and their importance for decompressional melting in eclogites. Eur J Mineral 7:1421-1436

Franz G, Spear FS (1983) High pressure metamorphism of siliceous dolomites from the central Tauern Window, Austria. Amer J Sci 283A:396-413

Frei D, Liebscher A, Franz G, Dulski P (2004) Trace element geochemistry of epidote minerals. Rev Mineral Geochem 56:553-605

Getty SR, Selverstone J (1994) Stable isotopic and trace element evidence for restricted fluid migration in 2 GPa eclogites. J Metamorphic Geol 12:747-760

Ghent ED, Black PM, Brothers RN, Stout MZ (1987) Eclogites and associated albite-epidote-garnet paragneisses between Yambe and Cape Colnett, New Caledonia. J Petrol 28:627-643

Gibbons W, Gyopari M (1986) A greenschist protolith for blueschist in Anglesey, U.K. *In*: Blueschists and Eclogites. BE Evans, EH Brown, (eds) Geol Soc Amer Memoir 164, p 217-228

Gieré R, Sorensen SS (2004) Allanite and other REE-rich epidote-group minerals. Rev Mineral Geochem 56: 431-494

Gomez-Pugnairea MT, Visonab D, Franz G (1985) Kyanite, margarite and paragonite in pseudomorphs in amphibolitized eclogites from the Betic Cordilleras, Spain. Chem Geol 50:129-141

Goto A, Banno S, Higashino T, Sakai C (2002) Occurrence of calcite in Sanbagawa pelitic schists: Implications for the formation of garnet, rutile, oligoclase, biotite and hornblende. J Metamorphic Geol 20:255-262

Grapes RH, Hoskin PWO (2004) Epidote group minerals in low–medium pressure metamorphic terranes. Rev Mineral Geochem 56:301-345

Heinrich CA (1982) Kyanite-eclogite to amphibolite facies evolution of hydrous mafic and pelitic rocks, Adula Nappe, Central Alps. Contrib Mineral Petrol 81:30-38

Hickmott DD, Sorensen SS, Rogers PSZ (1992) Metasomatism in a subduction complex: constraints from microanalysis of trace elements in minerals from garnet amphibolite from the Catalina Schist. Geology 20:347-350

Higashino T (1990) The higher-grade metamorphic zonation of the Sambagawa metamorphic belt in central Shikoku, Japan. J Metamorphic Geol 8:413-423

Higashino T, Sakai C, Kurata H, Enami M, Hosotani H, Enami M, Banno S (1984) Electron microprobe analyses of rock-forming minerals from the Sanbagawa metamorphic rocks, Shikoku Part II. Sazare, Kotu and Bessi areas. Sci Rept Kanazawa Univ 29:37-64

Higashino T, Sakai C, Otsuki M, Itaya T, Banno S (1981) Electron microprobe analyses of rock-forming minerals from the Sanbagawa metamorphic rocks, Shikoku Part I. Asemi River area. Sci Rept Kanazawa Univ 26:73-122

Hirajima T, Wallis SR, Zhai M, Ye K (1993) Eclogitized metagranitoid from the Su-Lu ultra-high pressure (UHP) province, eastern China. Proc Japan Acad, Ser B 68:249-254

Hirajima T, Zhang R, Li J, Cong B (1992) Petrology of the nyböite-bearing eclogite in the Donghai area, Jiangsu province, eastern China. Mineral Mag 56:37-46

Holland TJB, Powell R (1990) An enlarged and updated internally consistent thermodynamic dataset with uncertainties and correlations: The system K_2O-Na_2O-CaO-MgO-MnO-FeO-Fe_2O_3-Al_2O_3-TiO_2-SiO_2-C-H_2-O_2. J Metamorphic Geol 8:89-124

Holland TJB, Powell R (1998) An internally consistent thermodynamic data set for phases of petrological interest. J Metamorphic Geol 16:309-343

Hoscheck G (2001) Thermobarometry of metasediments and metabasites from the Eclogite zone of the Hohe Tauern, Eastern Alps, Austria. Lithos 59:127-150

Itaya T (1981) Carbonaceous material in pelitic schists of the Sanbagawa metamorphic belt in central Shikoku, Japan. Lithos 14:215-244

Itaya T, Brothers RN, Black PM (1985) Sulfides, oxides and sphene in high-pressure schists from New Caledonia. Contrib Mineral Petrol 91:151-162

Jayko AS, Blake MCJ, Brothers RN (1986) Blueschist metamorphism of the eastern Franciscan belt, northern California. *In*: Blueschists and Eclogites. BE Evans, EH Brown, (eds) Geol Soc Am Memoir 164, p 107-123

Korsakov AV, Shatsky VS, Sobolev NV, Zayachokovsky AA (2002) Garnet-biotite-clinozoisite gneiss: A new type of diamondiferous metamorphic rock from the Kokchetav Massif. Eur J Mineral 14:915-928

Kretz R (1983) Symbols for rock-forming minerals. Am Mineral 68:277-279

Krogh EJ (1982) Metamorphic evolution of Norwegian country-rock eclogites, as deduced from mineral inclusions and compositional zoning in garnets. Lithos 15:305-321

Krogh EJ, Oh CW, Liou JG (1994) Polyphase and anticlockwise *P-T* evolution for Franciscan eclogites and blueschists from Jenner, California, USA. J Metamorphic Geol 12:121-134

Kunugiza K, Takasu A, Banno S (1986) The origin and metamorphic history of the ultramafic and metagabbro bodies in the Sanbagawa metamorphic belt. *In*: Blueschists and Eclogites. BE Evans, EH Brown, (eds) Geol Soc Am Memoir 164, p 375-385

Lee DE, Thomas HH, Marvin RF, Coleman RG (1964) Isotopic ages of glaucophane schists from the area of Cazadero, California. US Geol Surv Prof Paper 475-D:105-107

Liou JG (1973) Synthesis and stability relations of epidote $Ca_2Al_2FeSi_3O_{12}(OH)$. J Petrol 14:381-413

Liou JG (1993) Stabilities of natural epidotes. Abhand Geol Bund 49:7-16
Liou JG, Maruyama S (1987) Paragenesis and compositions of amphiboles from Franciscan jadeite-glaucophane type facies series metabasites at Cazadero, California. J Metamorphic Geol 5:371-395
Liou JG, Maruyama S, Cho M (1987) Very low-grade metamorphism of volcanic and volcaniclastic rocks - mineral assemblages and mineral facies. *In*: Very Low-Grade Metamorphism. M Frey, (ed) Blackie Publishing Co., p 59-113
Liou JG, Zhang RY (2002) Ultrahigh-pressure metamorphic rocks. Ency Phys Sci Tech (Third Edition). 17, Academia Press, p 227-244
Maruyama S, Cho M, Liou JG (1986) Experimental investigations of blueschist-greenschist transition equilibria: pressure dependence of Al_2O_3 contents in sodic amphiboles - a new geobarometer. *In*: Blueschists and Eclogites. BW Evans, EH Brown, (eds) Geol Soc Am Memoir 164, p 1-16
Maruyama S, Liou JG (1987) Clinopyroxene-a mineral telescoped through the processes of blueschist facies metamorphism. J Metamorphic Geol 5:529-552
Maruyama S, Liou JG (1988) Petrology of Franciscan metabasites along the jadeite-glaucophane type facies series, Cazadero, California. J Petrol 29:1-37
Maruyama S, Liou JG, Terabayashi M (1996) Blueschists and eclogites of the world and their exhumation. Inter Geol Rev 38:485-594
Massonne HJ, O'Brien P (2003) Reviews of representative UHPM terranes: The Bohemian Massif and the NW Himalaya. *In*: Ultra-High Pressure Metamorphism. Notes in Mineralogy 5. DA Carswell, R Compagnoni, (eds) Eur Mineral Union, p 145-188
Masuda A, Nakamura N, Tanaka T (1973) Fine structures of mutually normalized rare-earth patterns of chondrits. Geochim Cosmochim Acta 37: 239-248
Mattinson CG, Zhang RY, Tsujimori T, Liou JG (in review) Epidote-rich talc-kyanite-phengite eclogites, Sulu terrane, eastern China. Am Mineral
Miyajima H, Matsubara S, Miyawaki R, Hirokawa K (2003) Niigataite, $CaSrAl_3(Si_2O_7)(SiO_4)O(OH)$: Sr-analogue of clinozoisite, a new member of the epidote group from the Itoigawa-Ohmi district, Niigata Prefecture, central Japan. J Mineral Petrol Sci 98:118-129
Miyashiro A (1994) Metamorphic Petrology. UCL Press, London, p 404
Miyashiro A, Banno S (1958) Nature of glaucophanitic metamorphism. Am J Sci 256:97-110
Miyashiro A, Seki Y (1958) Enlargement of the composition field of epidote and piemontite with rising temperature. Am J Sci 256:423-430
Moore DE (1984) Metamorphic history of a high-grade blueschist exotic block from the Franciscan complex, California. J Petrol 25:126-150
Moore DE, Blake MCJ (1989) New evidence for polyphase metamorphism of glaucophane schist and eclogite exotic blocks in the Franciscan Complex, California and Oregon. J Metamorphic Geol 7:211-228
Morrison J (2004) Stable and radiogenic isotope systematics in epidote group minerals. Rev Mineral Geochem 56:607-628
Nagasaki A, Enami M (1998) Sr-bearing zoisite and epidote in ultra high-pressure (UHP) metamorphic rocks from the Su-Lu province, eastern China: an important Sr-reservoir under UHP conditions. Am Mineral 83:240-247
Nakajima T (1982) Phase relations of pumpellyite-actinolite facies metabasites in the Sanbagawa metamorphic belt in central Shikoku, Japan. Lithos 15:267-280
Nakajima T, Banno S, Suzuki T (1977) Reactions leading to the disappearance of pumpellyite in low-grade metamorphic rocks of the Sanbagawa metamorphic belt in central Shikoku, Japan. J Petrol 18:263-284
Newton RC, Kennedy GC (1963) Some equilibrium reactions in the join $CaAl_2Si_2O_8$-H_2O. J Geophys Res 68: 2967 - 2983
Oberhänsli R (1986) Blue amphiboles in metamorphosed Mesozoic mafic rocks from the central Alps. *In*: Blueschists and Eclogites. BE Evans, EH Brown, (eds) Geol Soc Amer Mem 164, p 239-247
O'Brien PJ (1993) Partially retrograded eclogites of the Münchberg Massif, Germany; records of a multi-stage Variscan uplift history in the Bohemian Massif. J Metamorphic Geol 11:241-260
Oh CW, Liou JG (1990) Metamorphic evolution of two different eclogites in the Franciscan Complex, California, USA. Lithos 25:41-53
Oh CW, Liou JG, Maruyama S (1991) Low-temperature eclogites and eclogitic schists in Mn-rich metabasites in Ward Creek, California; Mn and Fe effects on the transition between blueschist and eclogite. J Petrol 32:275-301
Okamoto K, Maruyama S (1999) The high-pressure synthesis of lawsonite in the MORB+H_2O system. Am Mineral 84:362-373
Okay AI (1995) Paragonite eclogites from Dabie Shan, China: re-equilibration during exhumation? J Metamorphic Geol 13:449-460

Otsuki M (1980) Petrological study of the basic Sanbagawa metamorphic rocks in central Shikoku, Japan. Doctoral Dissertation, University of Tokyo, Tokyo, p 286
Otsuki M, Banno S (1990) Prograde and retrograde metamorphism of hematite-bearing basic schists in the Sanbagawa belt in central Shikoku. J Metamorphic Geol 8:425-439
Philippot P, Rumble ID (2000) Fluid-rock interactions during high-pressure and ultrahigh-pressure metamorphism. Inter Geol Rev 42:312-327
Poli S, Schmidt MW (2004) Experimental subsolidus studies on epidote minerals. Rev Mineral Geochem 56: 171-195
Potel S, Schmidt ST, de Capitani C (2002) Composition of pumpellyite, epidote and chlorite from New Caledonia - How important are metamorphic grade and whole-rock composition? Schweiz Mineral Petrogr Mitt 82:229-252
Raith M (1976) The Al-Fe(III) epidotes miscibility gap in a metamorphic profile through the Pennnine series of Tauern, Austria. Contrib Mineral Petrol 57:99-117
Reinecke T (1991) Very-high-pressure metamorphism and uplift of coesite-bearing metasediments from the Zermatt-Saas zone, Western Alps. Eur J Mineral 3:7-17
Reinecke T (1998) Prograde high- to ultrahigh-pressure metamorphism and exhumation of oceanic sediments at Lago di Cignana, Zermatt-Saas Zone, Western Alps. Lithos 42:147-189
Rolfo F, Compagnoni R, Xu S, Jiang L (2000) First report of felsic whiteschist in the ultrahigh-pressure metamorphic belt of Dabie Shan, China. Eur J Mineral 12:883-898
Rumble D, Giorgis D, Ireland T, Zhang Z, Xu H, Yui TF, Yang J, Xu Z, Liou JG (2002) Low $\delta^{18}O$ zircons, U-Pb dating, and the age of the Qinglongshan oxygen and hydrogen isotope anomaly near Donghai in Jiangsu Province, China. Geochim Cosmochim Acta 66:2299-2306
Rumble D, Wang Q, Zhang R (2000) Stable isotope geochemistry of marbles from the coesite UHP terrains of Dabieshan and Sulu, China. Lithos 52:79-95
Rumble D, Yui TF (1998) The Qinglongshan oxygen and hydrogen isotope anomaly near Donghai in Jiangsu Province, China. Geochim Cosmochim Acta 62:3307-3321
Sakai C, Higashino T, Enami M (1984) REE-bearing epidote from Sanbagawa pelitic schists, central Shikoku, Japan. Geochem J 18:45-53
Schmidt MW, Poli S (1994) The stability of lawsonite and zoisite at high pressures: Experiments in CASH to 92 kbar and implications for the presence of hydrous phases in subducted lithosphere. Earth Planet Sci Lett 124:105-118
Schmidt MW, Poli S (1998) What causes the position of the volcanic front? Experimentally based water budget for dehydrating slabs and consequences for arc magma generation. Earth Planet Sci Lett 163:361-379
Selverstone J, Franz G, Thomas S, Getty S (1992) Fluid variability in 2 GPa eclogites as an indicator of fluid behavior during subduction. Contrib Mineral Petrol 112:341-357
Selverstone J, Spear FS (1985) Metamorphic P-*T* paths from pelitic schists and greenstones in the southwest Tauern Window, Eastern Alps. J Metamorphic Geol 3:439-465
Shibakusa H, Maekawa H (1997) Lawsonite-bearing eclogitic metabasites in the Cazadero area, northern California. Mineral Petrol 61:163-180
Sobolev NV, Shatsky VS (1990) Diamond inclusions in garnets from metamorphic rocks; a new environment for diamond formation. Nature 343:742-746
Sorensen SS (1986) Petrologic and geochemical comparison of the blueschist and greenschist units of the Catalina schist terrane, southern California. *In*: Blueschists and Eclogites. BE Evans, EH Brown, (eds) Geol Soc Am Memoir 164, p 59-75
Sorensen SS, Grossman JN (1989) Enrichment of trace elements in garnet amphibolites from a paleo-subduction zone: Catalina Schist, southern California. Geochim Cosmochim Acta 53:3155-3177
Spear FS (1993) Metamorphic Phase Equilibria and Pressure-Temperature-Time Paths. Mineral Soc Amer Monograph, Washington, D.C., p 799
Spear FS, Franz G (1986) *P-T* evolution of metasediments from the eclogite zone, South-Central Tauern Window, Austria. Lithos 19:219-234
Strens RGJ (1965) Stability and relations of the Al-Fe epidotes. Mineral Mag 35:464-475
Tagiri M (1985) A comparison of graphitizing-degree and metamorphic zones of the Sanbagawa metamorphic belt in central Shikoku. J Japan Assoc Mineral Petrol Econ Geol 80:503-506
Takasu A (1989) *P-T* histories of peridotite and amphibolite tectonic blocks in the Sambagawa metamorphic belt, Japan. *In*: The Evolution of Metamorphic Belts. JS Daly, RA Cliff, BWD Yardley, (eds) Blackwell Scientific Publications, Oxford, p 533-538
Thurston SP (1985) Structure, petrology, and metamorphic history of the Nome Group blueschist terrane, Salmon Lake area, Seward Peninsula, Alaska. Geol Soc Am Bull 96:600-617
Vrána S, Gryda J (2003) Ultrahigh-pressure grossular-rich garnetite from the Moldanubian Zone, Czech Republic. Eur J Mineral 15:43-54

Wallis S, Aoya M (2000) A re-evaluation of eclogite facies metamorphism in SW Japan: Proposal for an eclogite nappe. J Metamorphic Geol 18:653-664

Wallis S, Takasu A, Enami M, Tsujimori T (2000) Eclogite and related metamorphism in the Sanbagawa belt, Southwest Japan. Bull Res Inst Nat Sci, Okayama Univ Sci 26:3-17

Yang JJ, Enami M (2003) Chromian dissakisite-(Ce) in a garnet lherzolite from the Chinese Su-Lu UHP metamorphic terrane: Implications for Cr incorporation in epidote minerals and recycling of REE into the Earth's mantle. Am Mineral 88: 604-610

Yao Y, Cong B, Wang Q, Ye K, Liu J (2000) A transitional eclogite- to high pressure granulite-facies overprint on coesite-eclogite at Taohang in the Sulu ultrahigh-pressure terrane, eastern China. Lithos 52: 109-120

Yoder HS (1955) Role of water in metamorphism. Geol Soc Am Spec Pap 62: 505-523

Yokoyama K (1976) Finding of plagioclase-bearing granulite from the Iratsu epidote amphibolite mass in central Shikoku. J Geol Soc Japan 82: 549-551

Yokoyama K, Brothers RN, Black PM (1986) Regional eclogite facies in the high-pressure metamorphic belt of New Caledonia. *In*: Blueschists and Eclogites. BE Evans, EH Brown, (eds) Geol Soc Am Memoir 164, p 407-423

Yoshizawa H (1984) Notes on petrography and rock-forming mineralogy; (16), Sector-zoned epidote from Sanbagawa Schist in central Shikoku, Japan. J Japan Assoc Mineral Petrol Econ Geol 79: 101-110

Yui TF, Rumble D, Lo CH (1995) Unusually low $\delta^{18}O$ ultra-high-pressure metamorphic rocks from the Sulu-terraine, eastern China. Geochim Cosmochim Acta 59: 2859-2864

Yui TF, Rumble D, Chen CH, Lo CH (1997) Stable isotope characteristics of eclogites from the ultra-high-pressure metamorphic terrain, east-central China. Chem Geol 137:135-147

Zhang RY (1992) Petrogenesis of high pressure metamorphic rocks in the Su-Lu and Dianxi regions, China. Ph. D. Thesis, Kyoto University, p 176

Zhang RY, Hirajima T, Banno S, Cong B, Liou JG (1995a) Petrology of ultrahigh-pressure rocks from the southern Su-Lu region, eastern China. J Metamorphic Geol 13:659-675

Zhang RY, Liou JG (1994) Coesite-bearing eclogite in Henan Province, central China: detailed petrography, glaucophane stability and PT-path. Eur J Mineral 6:217 - 233

Zhang RY, Liou JG (1997) Partial transformation of gabbro to coesite-bearing eclogite from Yangko, the Sulu terrane, eastern China. J Metamorphic Geol 15:183-202

Zhang RY, Liou JG, Cong B (1995b) Talc-, magnesite- and Ti-clinohumite-bearing ultrahigh-pressure metamafic and ultramafic complex in the Dabie Mountains, China. J Petrol 36:1011-1037

Zhang RY, Liou JG, Ernst WG (1995c) Ultrahigh-pressure metamorphism and decompressional *P-T* paths of eclogites and country rocks from Weihai, eastern China. Isl Arc 4:293-309

Zhang RY, Liou JG, Ernst WG, Coleman RG, Sobolev NV, Shatsky VS (1997) Metamorphic evolution of diamond-bearing and associated rocks from the Kokchetav Massif, northern Kazakhstan. J Metamorphic Geol 15:479-496

Zhang RY, Liou JG, Katayama I (2002) Petrologic characteristics and metamorphic evolution of diamond-bearing gneiss from Kumdy-kol. *In*: The Diamond-bearing Kokchetav Massif, Kazakhstan: Petrochemistry and Tectonic Evolution of an Unique Ultrahigh-Pressure Metamorphic Terrane. CD Parkinson, I Katayama, JG Liou, S Maruyama, (eds) Universal Academy Press, Inc., Tokyo, p 213-234

Zhang RY, Liou JG, Zhang YF, Fu B (2003) Transition of UHP eclogites to gneissic rocks of low-grade amphibolite facies during exhumation: Evidence from the Dabie terrane, central China. Lithos 70:269-291

Zhang RY, Liou JG, Zheng JP (2004) Ultrahigh-pressure corundum-rich garnetite in garnet peridotite, Sulu terrane, China. Contrib Mineral Petrol 146:21-31

Zheng YF, Cong B, Li S (1996) Extreme ^{18}O depletion in eclogite from the Su-lu terrane in east China. Eur J Mineral 8:317-323

Zheng YF, Fu B, Gong B, Li L (2003) Stable isotope geochemistry of ultrahigh pressure metamorphic rocks from the Dabie–Sulu orogen in China: implications for geodynamics and fluid regime. Earth Sci Rev 62: 105-161

Zheng YF, Li Y, Gong B, Fu B, Xiao Y (1999) Hydrogen and oxygen isotope evidence for fluid-rock interactions in the stages of pre- and post-UHP metamorphism in the Dabie Mountains. Lithos 46:677-693